Development of a novel screen protocol for the identification of genes causing replication associated genomic instability in *Schizosaccharomyces pombe*

by

Morgan L. Jarvis

A thesis submitted to the Department of Pathology
in conformity with the requirements for the degree of Master of Science

Queen's University
Kingston, Ontario, Canada

May 2008

Abstract

Replication fork stalling is a source of potentially tumourigenic genomic instability. The RecQ family helicase, Rqh1, is critical for the prevention of replication fork collapse and the formation of potentially deleterious recombination intermediates following fork stalling. Previous work in our lab with *Schizosaccharomyces pombe* (fission yeast) has shown that $rqh1^{0}/rqh1^{0}$ diploids are inherently unstable and show rapid reversion to the haploid state. The current work exploits this characteristic of fission yeast $rqh1^{0}$ mutants in a screen for genes that normally promote replication associated genomic instability. The $rqh1^{0}rad3^{0}$ mutant strains employed in this work incorporate the checkpoint deficiency caused by a lack of Rad3, so as to exacerbate the genomically unstable nature of this model. The current work describes the lithium acetate transformation based random mutagenesis by non-homologous integration of the $ura4^{+}$ selectable marker into the $rqh1^{0}rad3^{0}$ fission yeast strains. This random mutagenesis generated extensive (24,500 – 50,000) mutant libraries. The quality of the libraries was assessed by *can1* mutant assay, confirming an adequately extensive mutagenesis for the proposed screen. The process to be employed in the screen would involve the crossing of the mutant libraries, with the hope of generating diploids that will have two mutant copies of the same gene. Some of these diploids would appear unusually stable, showing a normal sporulation phenotype. This would indicate the mutation of a gene that normally promotes genomic instability following replication fork stalling. The practicality of the proposed screen of a vast number of diploids was assessed and described in detail in the current work. A technique involving inverse PCR (IPCR) adopted from previous work to identify mutants of interest, was also investigated. The investigation of this technique, and the work of others, suggests that transformation using such selectable marker

fragments results in most apparent transformants containing extrachromosomal *ura4*$^{+}$ fragments. These fragments are thought to provide the predominant template for IPCR, rendering the process unsuccessful at identifying the mutation in the current screen. However, with the mutant libraries generated, and the screen procedure detailed, the stage is set to conduct the screen once a more appropriate mutation location technique is identified.

Acknowledgements

I would like to thank my supervisor, Dr. Scott Davey, for taking me into his lab and guiding me through this project. I would also like to thank the members of the Davey lab for their support and guidance, especially Kathy Kennedy and Nicole Archer for their technical expertise.

Table of Contents

List of Tables

List of Figures

List of Abbreviations

9-1-1	Rad9-Rad1-Hus1
A	adenine
ATM	ataxia telangiectasia mutated
ATR	ataxia telangiectasia mutated and Rad3 related
ATRIP	ataxia telangiectasia mutated and Rad3 related interacting protein
BER	base excision repair
BRCA	breast cancer associated gene
Cdc	cell division cycle
Chk	checkpoint kinase
DNA	deoxyribonucleic acid
E. coli	*Escherichia coli*
EDTA	ethylenediaminetetraacetic acid
hus	hydroxyurea sensitive
IPCR	inverse PCR
L	leucine
NER	nucleotide excision repair
PCNA	proliferating cell nuclear antigen
PCR	polymerase chain reaction
PIKK	phosphoinositide 3-kinase related kinase
PM	minimal media
Rad	radiation sensitive
RFC	replication factor C
rpm	revolutions per minute
S. pombe	*Schizosaccharomyces pombe*
SPA	sporulation medium
U	uracil
UV	ultraviolet
YE	yeast extract medium
YES	yeast extract medium supplemented with adenine, leucine, and uracil

Chapter 1: Introduction

1.1 *Schizosaccharomyces pombe* and cell cycle checkpoints:

Schizosaccharomyces pombe (fission yeast) has provided an excellent model for study of the cell cycle, checkpoint control, and DNA damage and repair mechanisms. It is a single-celled free living archiascomycete fungus sharing many features with cells of higher eukaryotes (1). With a 13.8 Mb genome (1) and less than 5000 genes (1), and a short life cycle, fission yeast provides an easily manipulated laboratory tool for the study of human disease (1, 2). Understanding of the molecular and biochemical basis of cellular function tends to progress simultaneously in budding and fission yeast, as it is generally accepted that if genes are shared between these genetically diverse fungi, then they are common among all eukaryotes (2, 3). The understanding of the cell cycle and its control in the face of damaged DNA or threat of genomic instability is no exception to this rule, with work progressing simultaneously in both yeasts and human cell lines. The focus organism in the current study is fission yeast, with implication to the understanding of the molecular basis of human cancer.

The cell cycle is an orderly process undertaken by each cell to reproduce its genome during the normal growth and development of the organism. The stages of the cell cycle involve DNA replication (S-phase) and sister chromatid segregation (mitosis), separated by gap phases where errors in the genome are detected and corrected. The cell cycle is controlled by positive and negative regulatory biochemical pathways. The cell cycle checkpoints are considered negative biochemical regulators that involve detection of DNA damage. Detection is followed by the generation of a signal that is amplified and transmitted to the cell cycle machinery, resulting in transient arrest of the cell cycle. In this fashion, the progression of the cell cycle is delayed if the integrity of the genome is

compromised, either as a consequence of normal cellular processes or environmental factors (3, 4). Cell cycle arrest occurs at several distinct points in the cell cycle, indicating the work of checkpoints. These have traditionally been labeled the G1/S, Intra-S, G2/M, and DNA replication checkpoints, which prevent DNA replication and mitosis in the presence of damaged or unreplicated DNA (4, 5). The current work involves the manipulation of mechanisms underlying the Intra-S and DNA replication checkpoints.

The delay in the cell cycle in response to DNA damage or replication defects allows for damage repair, and is therefore critical for the maintenance of genomic stability. Loss of checkpoint function can lead to transmission of damaged or partially unreplicated DNA to daughter cells, resulting in chromosomal rearrangements, amplification, and loss (hallmarks of cancer cells) (5). For instance, 25-50% of human adenocarcinomas have been shown to contain more than nine chromosomal alterations (6). It has then been proposed that these chromosomal alterations are a reflection of a much greater number of smaller mutations, like single base substitutions or deletions and additions of a few nucleotides (7, 8, 9). To account for the large number of mutations in cancer cells, the “mutator phenotype” hypothesis has been proposed (10, 11, 12). This theory recognizes the importance of the cell cycle checkpoints, since spontaneous mutations in such genome-stability genes are considered the basis for neoplastic transformation. An initial mutation in a genome-stability gene (eg. DNA polymerases, DNA repair enzymes, DNA damage checkpoint control and chromosome segregation) either inherited or arising from some mutagenic event, leads to a state of hyper-mutagenesis, resulting in a cascade of additional random mutations (13, 14). This theory becomes particularly powerful when combined with a Darwinian approach to selection of mutations giving a growth advantage (15, 16). It explains the stepwise nature of

carcinogenesis where individual mutations are responsible for each stage in the progress of a cell from normal somatic cell to malignancy, all starting with the propensity to generate new mutations caused by a defective genome-stability gene (like those involved in cell cycle checkpoints). The role of multiple mutations in tumourigenesis has been most discussed in colorectal cancer, where the high rate of cell division in epithelial cells may allow for enough random mutations to lead to neoplastic transformation without the mutator phenotype. However, the low spontaneous rate of mutagenesis of somatic cells (1.4×10^{-10} nucleotides/cell/division or 2×10^{-7} mutations/gene/cell division (14)) and the very large number of mutations accumulated in tumours (estimated to be as high as 10^{12} or more (17)), means that tumourigenesis in less rapidly dividing tissue would require the instability generating mutator phenotype (14, 15, 18). In considering the vast number of mutations that typically accumulate in cancer cells, it is important to note that only a small number are actually required for the initiation of carcinogenesis. It has been proposed that as few as 4-7 (or less) genetic hits are enough for carcinogenesis, as long as the affected genes include “gatekeepers” and “caretakers” (19, 20).

Several of the checkpoint genes have been associated with human cancers: *HRad17* is a potential diagnostic tool due to its observed overexpression in lung and breast cancer (21, 22), mutations of *BRCA1* in breast and ovarian cancer (23, 24, 25), *BRCA2* in breast cancer (26), *CHK2* in Li-Fraumeni Syndrome (predisposition to a variety of cancers) (27, 28), *ATM* in ataxia telangiectasia (AT) with effects including extreme sensitivity to ionizing radiation and cancer predisposition (29, 30, 31, 32), and most significantly, the “cellular gatekeeper for growth and division”, *p*53 (33), which has been associated with over 50% of human cancers (33, 34). Also implicated in cancer, and working closely with the cell cycle checkpoints are the DNA damage repair pathways:

Xeroderma pigmentosum is seen in nucleotide excision repair (NER) deficient individuals (35), and hereditary and sporadic forms of colon cancer in DNA mismatch repair (MMR) individuals (36, 37, 38, 39, 40). To further illustrate the significance of these pathways in human cancer, it is useful to consider a classification of the kinds of genes that have been found to contribute to cancer when they are mutated (more than 1% of all genes in the human genome (41)), noting that cell cycle control and repair pathways constitute a major part of this list: a) genes encoding growth factors and growth factor receptors; b) genes participating in signal transduction and otherwise in the cell cycle; c) transcription-controlling genes and other genes encoding nuclear proteins; d) genes involved in DNA repair and chromosomal replication, mitotic segregation and telomere maintenance; e) genes responsible for triggering apoptosis of abnormal cells; and f) genes involved in interactions of cells with the extra-cellular matrix and blood vessels (42).

1.2 The checkpoint proteins:

Traditionally, checkpoints were thought of as specific points in the cell cycle where DNA integrity was assessed before allowing the cell cycle to continue (43). However, recent research has suggested that the checkpoints are not restricted to specific points (such as phase transitions), but rather are found to act throughout the cell cycle (44). The checkpoints are best regarded as biochemical pathways that continuously monitor genome integrity, and in response to the state of the DNA, control the cell cycle. These signal transduction pathways can be thought of as being comprised of sensor, transducer, mediator/adaptor and effector elements. In response to DNA damage or blocked DNA replication, a signal is generated, amplified, and relayed to specific target molecules that arrest the cell cycle until the lesion is repaired (5). It is also important to recognize that cell cycle arrest is not the only function of these checkpoints (45). These

checkpoints also control the activation of DNA repair and the movement of repair proteins to damage sites (46, 47, 48, 49), transcriptional programs (3), telomere length (50) and apoptosis (51).

As previously mentioned, understanding of the checkpoints tends to progress simultaneously in mammals, budding and fission yeast. The following discussion therefore focuses on the elements common to all, using the terminology relevant to fission yeast, unless otherwise stated. Refer to Table 1 to cross-reference homologous proteins between organisms.

Since the proteins involved in regulating progression through the cell cycle are also involved in the checkpoint responses, it has been proposed that the DNA damage checkpoint response is the damage-induced amplification of a biochemical pathway that is operative under normal growth conditions (44, 52). The checkpoint response thus begins with detection of damaged DNA, where damage sensor proteins recognize specific aberrant DNA structures amongst an excess of related structures (undamaged DNA) (44). Such aberrant structures include single and double strand breakage, damaged bases, UV radiation induced cyclobutane pyrimidine dimers and (6-4) photoproducts, and most relevant to the current work, stalled and collapsed DNA replication forks (44, 53, 54).

Due to structural and sequence homology between the damage sensors Rad17 and the Rad9-Rad1-Hus1 (9-1-1) complex and the DNA replication complexes RFC and PCNA (55, 56), the known function of these replication proteins has been inferred on the DNA damage sensors. During replication, the RFC1-5 complex is considered a “clamp-loader” which binds to primed DNA and recruits the homotrimeric doughnut-ring-like PCNA (“clamp”) to form a sliding clamp that tethers DNA polymerases to the DNA template (57, 58). PCNA then acts to tether replication proteins (59).

Table 1: Selected checkpoint protein analogs in common model organisms.

Protein Function	**Fission yeast**	**Budding yeast**	**Mammals**
Sensors:			
RFC1-like	Rad17	Rad24	Rad17
PCNA-like	Rad9	Ddc1	Rad9
	Rad1		Rad1
	Hus1	Mec3	Hus1
Mediators:	Crb2	Rad9	BRCA1
	Rad4	Dpb11	TopBP1
	Mrc1	Mrc1	Claspin
Transducers:			
PI3-kinases (PIKK)	Rad3	Mec1	ATR
	Tel1	Tel1	ATM
PIKK binding partner	Rad26	Ddc2	ATRIP
Effector Kinases:	Chk1	Chk1	Chk1
	Cds1	Rad53	Chk2
Adaptor:	Mrc1	Mrc1	Claspin

Current understanding of Rad17 and 9-1-1 complex function fits this model. Rad17, which is chromatin-associated throughout the cell cycle (60), recruits the 9-1-1 complex to sites of DNA damage (61). The 9-1-1 complex then acts to tether signaling and repair molecules to the damage site (62, 63). Rad17 shares homology with all five subunits of RFC (replication factor C) (64). Interaction between Rad17 and the 9-1-1 complex has been shown in humans and fission yeast (65, 66), and after DNA damage the 9-1-1 complex becomes extraction resistant and chromatin-bound (67), suggesting that Rad17 ("clamp loader") loads the 9-1-1 complex ("clamp") onto sites of DNA damage.

The "sensor kinases" or transducers include Rad3 (ATR in mammals) and Tel1 (ATM in mammals) which are recruited by the 9-1-1 complex and act at the top of the checkpoint signaling pathways (68, 69). It has been proposed that signaling pathways responding to DNA damage can be divided into two basic types, stemming from the recognition of two basic molecular structures: Rad3/ATR in response to single strand DNA, and Tel1/ATM in response to double strand breaks (70). Interacting proteins include Rad26 which has been shown critical to mitotic arrest and forms a complex with Rad3. This heterodimer can bind DNA independently of the other checkpoint proteins (Hus1, Rad1, Rad9 and Rad17) (71). Rad26 shows Rad3 dependent phosphorylation following DNA damage and only Rad26 is required for Rad3 kinase activity (71, 72). The importance of Rad4 in the checkpoint signal initiation has also been demonstrated (62, 73). A complex of Rad9-Rad4 forms following Rad9 C-terminus phosphorylation, promoting the formation of a Rad3-Rad4 complex which acts as a signal initiator (62). Rad4 aids in bringing Crb2 and Chk1 into proximity of Rad3 in response to DNA damage, and Mrc1 during S-phase (recruiting Cds1 for activation by Rad3) (62). Substrates for phosphorylation by Rad3 are recruited independently of Rad3, perhaps by

Rad4 as mentioned above, and perhaps by the Rad17-RFC complex (74). Among the substrates phosphorylated by Rad3 are the adaptor proteins Crb2 (related to the breast and ovarian cancer associated genes BRCA1 and BRCA2 (75, 76)) and Mrc1 which lead to the activation (by Rad3) of downstream effector kinases Chk1 in response to DNA damage, and Cds1 in response to blocked DNA replication (76). The active effector kinases then control the cell cycle: Chk1 (activated by damage specific structures) and Cds1 (activated by replication specific structures) (77), phosphorylate Cdc25 which promotes its binding to 14-3-3 proteins, preventing it from activating Cdc2, thus preventing mitosis (78).

Rad3 is a protein kinase of 2396 amino acids, and has been found critical for checkpoint response to DNA damage (79, 80), S-phase arrest (77, 81), and the S-phase checkpoint (DNA damage signal via the intra-S checkpoint and aberrant replication forks via the replication checkpoint) (77, 81). The DNA damage checkpoints have actually been pin-pointed in the cell cycle by the observation of Rad3 phosphorylation of Chk1 in response to damage during late S-phase and G2, but not during G1/early S-phase or mitosis (82). It is also interesting to note that following DNA damage, Rad3 is only required to initiate the DNA damage checkpoint response, but following S-phase arrest, Rad3 is required to initiate and maintain the DNA replication checkpoint response, further demonstrating its importance in the current screen (82).

1.3 The S-phase checkpoints:

Of particular relevance to the current work is the way in which cells deal with aberrant replication forks during S-phase. As described above, the traditional view was that cells in S-phase activated one of two checkpoint pathways, one to signal DNA damage through the intra-S checkpoint, and the other in response to aberrant replication

forks through the replication checkpoint (70). However, although the signal pathway response to DNA damage and repair differs in certain aspects to the response to stalled replication forks (the purpose of which is to stabilize stalled forks and resume replication), the end result is the same: the cell cycle is arrested to prevent mitosis in the presence of damaged DNA or incomplete replication (70, 76, 83). It has thus been proposed that the two responses above can be integrated into one pathway, termed the S-phase checkpoint (70). It has also been suggested that this regulation of DNA replication by checkpoint controls may be the most important, since replication fork collapse leads to chromosome rearrangements (genome instability). These rearrangements can lead to altered gene expression, resulting in cancer if important mechanisms like the cell growth machinery are altered (as through the activation of oncogenes) (70).

Fidelity in DNA replication is critical to ensure the integrity of the genome passed to daughter cells. Thus, dealing with perturbations from intrinsic replication errors or external agents, is a challenging but important role of the replication machinery (76). The genome is especially vulnerable to mutation and destabilization during S-phase since strands are separated, leaving ssDNA exposed to mutagens (84). Replicational stress can be caused by malfunctioning replication machinery (85), blockage of replication fork progression by DNA damage (such as UV-induced lesions, adducts and abasic sites) or lack of dNTPs (84, 86). In dealing with these perturbations, the checkpoint machinery blocks cell cycle progression, downregulates later origin “firing”, stabilizes stalled replication forks and facilitates restart of collapsed forks (87). The Rad3-Cds1 pathway is largely responsible for this checkpoint response, and the stabilization of stalled replication forks is essential to ensure the continuation of replication without generating genomic instability (88). The purpose of stabilization is to maintain the replisome enzymes at the

site of DNA incorporation, and to protect the newly synthesized DNA ends, so that replication can continue when the problem is resolved (89). If replication forks are not stabilized, replication fork "collapse" results. This is where the replication proteins become dissociated from the DNA, generally resulting in strand breakage, and recombination is then required to resume replication (89).

The stabilization of stalled replication forks is the most critical stage in dealing with replication perturbations. Without being re-stabilized, the superhelical tension in the DNA ahead of the fork can cause it to regress so that the two nascent strands separate from their parental strands and pair with each other (a "reversed fork")(90). This structure is equivalent to a Holliday junction and is also known as a "chicken-foot" structure (Figure 1) (91). If this structure is not resolved by reverse branch migration, through the work of a RecQ family helicase, fork collapse can result (86). The broken strands of the collapsed fork are then resolved by potentially mutagenic recombination (86). The replication checkpoints overlap with the DNA damage checkpoints in this process. If replication forks are not stabilized by the Rad3 – Cds1 response, then the collapsed fork is treated as DNA damage, triggering the Rad3 – Chk1 response that ensures cell cycle arrest prior to mitosis, and damage repair (76, 82, 92, 93).

Cds1 has been found critical for the stabilization of stalled replication forks through its regulation of Mus81, Rad60, and Rqh1. Rqh1 is a RecQ related DNA helicase that acts at stalled replication forks to prevent the aberrant "chicken-foot" structure from forming, thus promoting polymerase association and inhibiting recombination by clearing structures that would be targets for nuclease cleavage (94). Mus81 forms a complex with Eme1 and is such a nuclease that targets these Holliday junction-like structures formed at

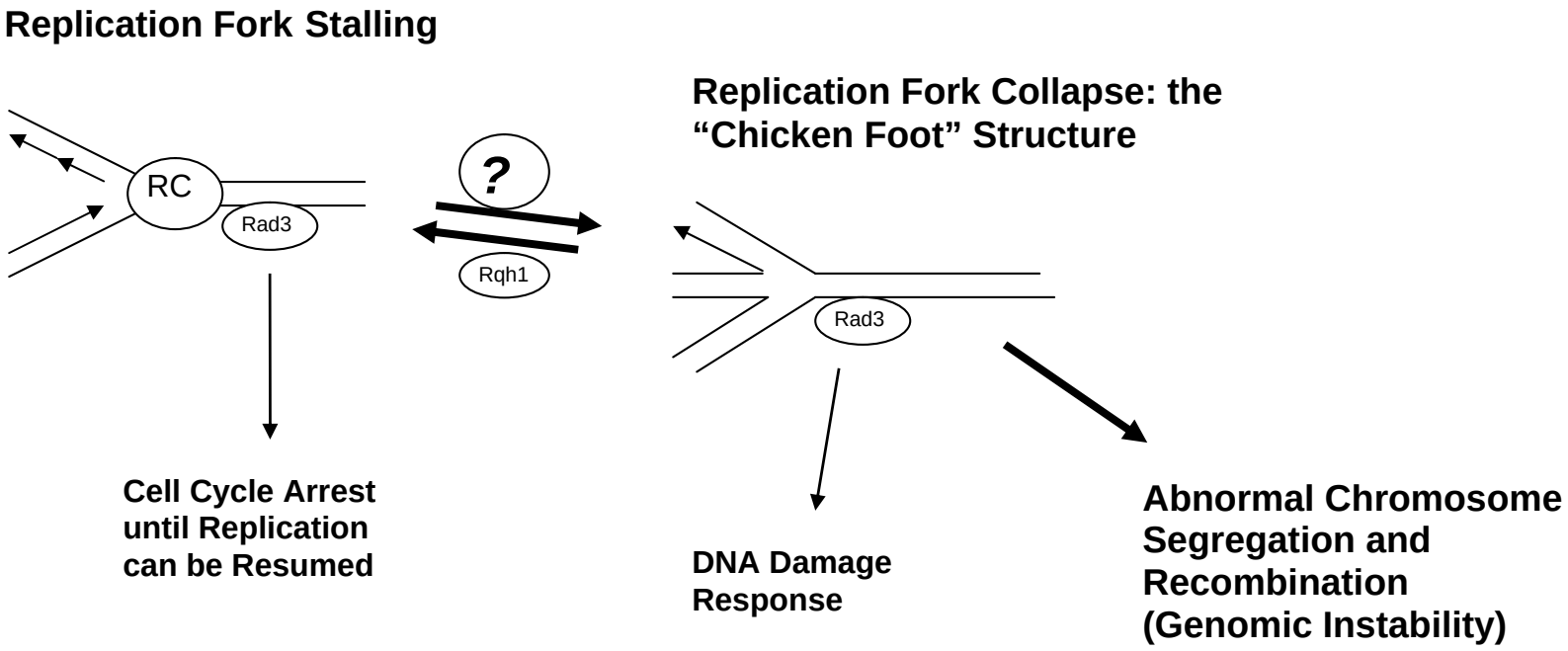
Replication Fork Stalling
RC
Rad3
?
Rqh1
Replication Fork Collapse: the
"Chicken Foot" Structure
Rad3
Cell Cycle Arrest
until Replication
can be Resumed
DNA Damage
Response
Abnormal Chromosome
Segregation and
Recombination
(Genomic Instability)

Figure 1A

Replication Fork Stalling

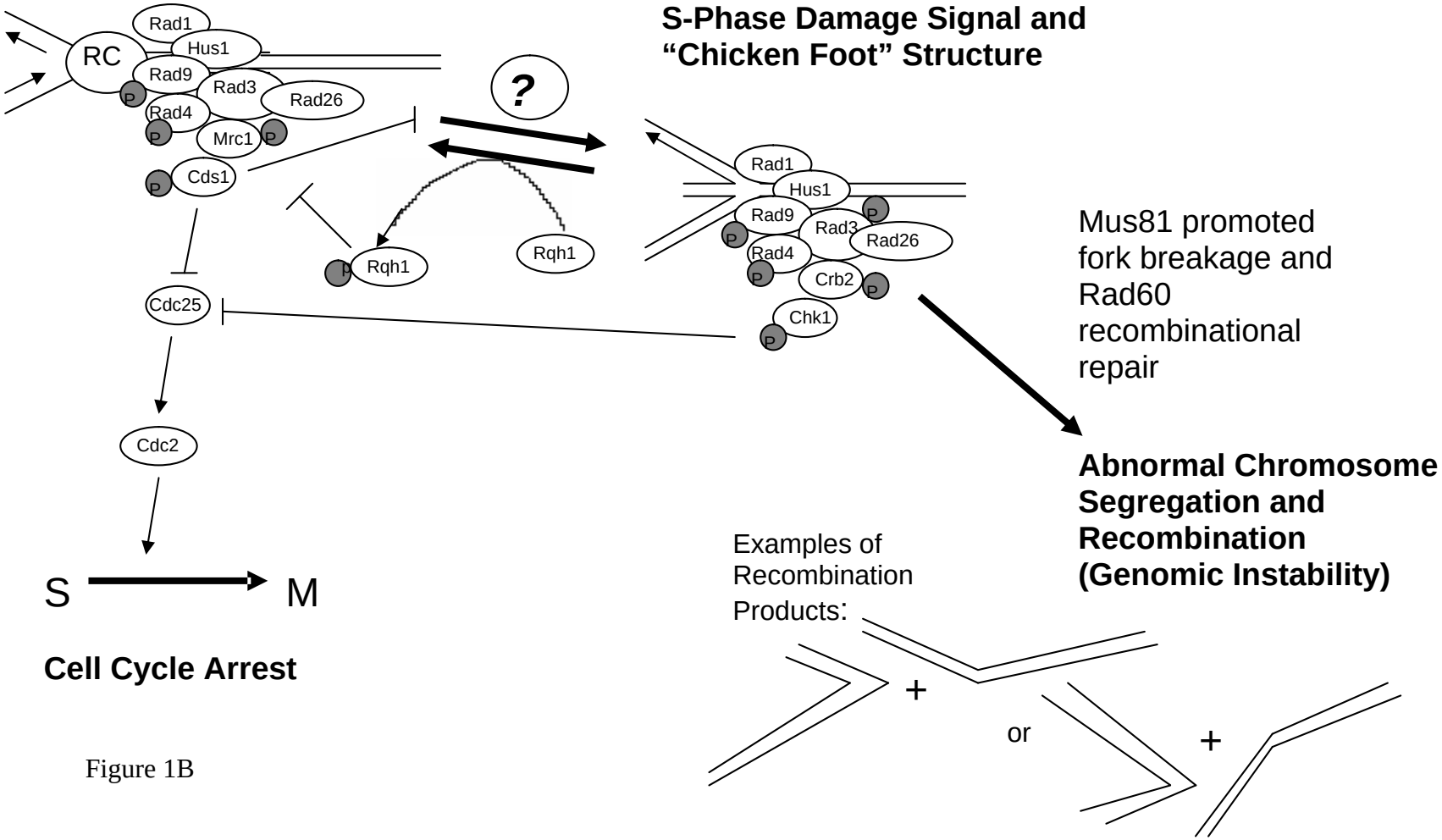

Figure 1B

Figure 1: Goal of the screen in the context of replication fork stalling and the associated signal transduction pathways. Figure 1A illustrates the screen target factors (denoted by "**?**") in the context of Rqh1 and Rad3 function in response to replication fork stalling and collapse. Figure 1B includes the checkpoint pathways associated with replication fork stalling and collapse.

stalled replication forks (95, 96). Rad60 is then required for recombinational-mediated repair of the replication-induced strand breaks (97). Thus, by facilitating the activity of Rqh1 (98), causing Mus81 dissociation from chromatin by phosphorylation (88), and inducing the nuclear delocalization of Rad60 (96), Cds1 prevents the generation of chromosomal rearrangement and potential genomic instability following stalled replication forks. Studies have shown that mutator phenotypes caused by mutations in replication genes are significantly exacerbated by mutations in Cds1 (85, 99). *rqh1*$^{-}$ show defects in chromosome segregation in mitosis following replication arrest induced by HU (84), and without exogenous insult to DNA (100). Rqh1 has also been found necessary to suppress inappropriate recombination by prevention of Holliday junctions (101). Mus81 is an evolutionarily conserved damage tolerance protein with an endonuclease domain (76), and interacts with Cds1 through its FHA (forkhead-associated) domain (102). The Cds1 FHA domain also associates with Rad60 in response to replication arrest (96). Mus81 is thought to be the eukaryotic Holliday junction resolvase, but has also been shown to process stalled replication forks by cleavage before regression to form Holliday junctions, especially in the absence of Sgs1 (Rqh1) function in budding yeast (103). It has thus been suggested that the RecQ and Mus81 pathways act independently at stalled replication forks to affect the same end of restarting replication (86). Double mutants of *rqh1* and *mus81* are nonviable, demonstrating the importance of each pathway to the resolution of stalled replication forks (104). It has also been shown in budding yeast, that the *sgs1* (*rqh1*) and *mus81* double mutant combined with a mutant homologous recombination gene such as *rad52* (*rad22* in fission yeast), results in the lethality being suppressed (95, 105), suggesting that the lethality caused by a lack of both pathways results from hyper-recombination leading to devastating genomic instability. The

resulting theory is that Rqh1 promotes the reversal of fork regression, preventing unscheduled recombination, whereas Mus81 promotes fork breakage to a polar double strand break, allowing the fork to restart by a recombinogenic “break-induced replication” pathway (89). A visual depiction of the roles of Cds1, Rqh1, Mus81, and Rad60 in the context of replication fork stalling and collapse, the associated checkpoint pathways, and the goal of this study, can be seen in Figure 1B.

The fission yeast protein Rqh1 is of particular relevance to the current work. Rqh1 has been found critical to recovery from S-phase arrest and in the toleration of DNA damage during S-phase (84, 98). Rqh1 is a 3’ to 5’ helicase and member of the RecQ family of DNA helicases, of which there are at least 16 members. The number of RecQ family helicases in each organism increases with complexity, from one in single celled organisms to at least 5 in humans (106). Rqh1 is homologous to Sgs1 in budding yeast, and BLM in humans (107, 108). The RecQ family in general, has been shown to process regressed replication forks to allow resumption of replication, with the universally conserved phenotype of cells lacking RecQ helicases being S-phase-specific hyper recombination (94). Included in this family are the human disease associated helicases BLM (Bloom’s syndrome), WRN (Werner’s syndrome), and the Rothmund-Thomson’s syndrome helicase (109, 110). All are associated with predisposition to malignancies with patients homozygous for mutations in *BLM* having increased rates of chromosomal rearrangement, chromosome breakage, sister chromatid exchange and recombination (111, 112). This predisposition to malignancy through demonstrated genomic instability is explained by the implication of the RecQ family helicases in the resetting of regressed forks to limit nonproductive recombination following fork cleavage (86, 108, 113, 114).

1.4 Rationale and hypothesis for the genomic instability screen:

Replication fork stalling and the need to stabilize the replication fork to prevent the generation of genomic instability is a regular occurrence in the cell, and of great importance to genomic integrity. Armed with the knowledge that Rqh1 plays a critical role in this process to prevent deleterious genetic alterations, and that this genomic instability in fission yeast *rqh1* mutants is expressed in an easily identifiable instability phenotype, it is proposed that an *rqh1*^{0} mutant strain would provide an ideal model in a screen for genes that normally cause replication associated genomic instability. Recalling the mutator phenotype hypothesis of cancer cells described above, the kind of instability generating genes potentially identified by this work are the kind of genes that could form the basis for a mutator phenotype. The work of such genes, in promoting deleterious chromosomal alterations following replication fork arrest, would normally be undone by Rqh1 in re-establishing regressed replication forks. Without Rqh1 function, it is thought that the work of these genes results in the observed genomic instability. It is thus proposed that a screen involving a genome wide random mutagenesis of cells lacking Rqh1 (*rqh1*^{0}) could be used to identify genes that normally promote replication associated genomic instability. Cells containing mutations in such a gene would no longer display the characteristic *rqh1*^{0} instability. This proposal is based on the knowledge that *rqh1*^{0}/*rqh1*^{0} diploids are normally highly unstable, showing reversion to the diploid state (preliminary work from our lab). It is also known that *rad3*^{0} mutants are defective in the DNA damage and replication checkpoints, and with blocked DNA synthesis cause irreversible damage (93). Therefore, adding this mutation to the *rqh1*^{0} mutation would result in a global instability phenotype. The mutants would not only be unable to recover

stalled replication forks to reinitiate replication without genomic rearrangement, but also lack the ability to trigger the checkpoint and arrest the cell cycle for damage repair.

The goal of the screen is to identify genes that normally promote genomic instability, so that when mutated, revert the highly unstable *rqh1*^{0}*rad3*^{0} strain to stability. Since a diploid phenotype is the basis for the screen, it is limited to situations where two null alleles of the same gene are combined in one diploid, or to haploinsufficient or dominant negative mutants. In order to identify mutants with two null alleles of the same gene in one diploid, a vast number of potential mutants must be screened. It is also noteworthy that this *rqh1*^{0}*rad3*^{0} strain has both a structural (*rqh1*^{0}) and regulatory (*rad3*^{0}) mutation, reducing the likelihood of false-positives from the screen. For instance, a suppressing mutation that simply slows the cell cycle should not suppress instability. It is also important that both of the mutations are gene disruptions, so that no intragenic event could revert the strain to stability. Possible findings of interest in this screen would be currently unknown genes responsible for the double strand breaks (DSBs) resulting from the formation of Holliday junctions ("chicken-foot" structure), following fork reversal during stalled replication. It is thought that repair of these DSBs is required to reestablish active replication forks, but is also part of the potentially deleterious generation of chromosomal rearrangements (93). Given the study mentioned above (Bastin-Shanower *et al.* - 105), where the *rqh1* and *mus81* double mutant was combined with a mutant recombination gene and the lethality of the double mutant was suppressed, it is possible that a mutation generated in *mus81*, *eme1*, or a recombination gene like *rad60*, could result in the generation of false positives from the screen. Refer to Figure 1 for a depiction of the goal of the screen in the context of signalling pathways associated with replication fork stalling and collapse.

It is proposed that the screen could be conducted by generating libraries of mutant *rqh1*^{0} cells (employing a genome-wide random mutagenesis technique), crossing the haploid libraries to form diploids, which are then screened for a stable phenotype (displaying normal sporulation). This is based on the knowledge that *rqh1*^{0}*/rqh1*^{0} diploids are highly unstable, and the proposal that any *[**?**gene]*^{0}*rqh1*^{0}*/[**?**gene]*^{0}*rqh1*^{0} diploids, or for dominant negative mutants: *[**?**gene]*^{0}*rqh1*^{0}*/rqh1*^{0} diploids, would show normal stability (where "***?***" is the unknown gene responsible for the generation of replication associated genomic instability as depicted in Figure 1). Upon generation of stable diploids containing the mutation of interest (in the "***?***" gene), identification of the gene of interest will be necessary. It is proposed that a technique involving inverse PCR (IPCR), as previously described (115), should be ideal for this purpose. The current work is thus a detailed investigation of the conditions required to perform this novel screen, after generating adequate mutant libraries, followed by attempts at the IPCR procedure required to identify mutants of interest.

1.5 Generation of mutant libraries:

Libraries of mutants in both mating types of *rad3*^{0}*rqh1*^{0} strains were generated in numbers such that every gene in the fission yeast genome could, theoretically, be knocked-out at least once in each library. Initially, an appropriate random mutagenesis method had to be employed to generate as many mutants in one round of mutagenesis as was physically manageable. In considering random mutagens, two different techniques for mutagenesis based on illegitimate recombination had potential for success in the current screen. One method involves non-homologous plasmid integration of a marked sequence, followed by rescue of the sequence, along with genomic DNA, back into the plasmid (116). Although illegitimate, the randomness of this mutagenesis method was not

directly addressed, so was not used in the current screen. The other relevant method was developed by Chua *et al.* (115) and involves the illegitimate integration of a linear marker sequence (*ura4*$^{+}$) into the genome. The genome has the innate *ura4*$^{+}$ sequence removed so that homology will not affect the randomness of integration, and to allow for the selection of successful transformants. Following the isolation of transformants, identification of the gene sequence directly adjacent to the insert is possible through inverse PCR (IPCR). This method was proven random and thought ideal for the current screen, where the identification of an unknown disrupted gene is desired, given their (115) success in implementing the procedure.

In generating the mutant libraries, it was necessary to know approximately how many transformants might be adequate to form a library with, at least theoretically, a mutant form of every gene in the fission yeast genome. Given the different size of different genes, and the varying susceptibility of various genes to integrate foreign DNA fragments, the calculations could only be broad approximations. It was therefore considered adequate to approximate the number of genes in the fission yeast genome to 5000, with approximately half of the genome being protein-coding (1), meaning that the chance of hitting any given gene in the random mutagenesis was 1/10,000. Theoretically, a library of at least 10,000 mutants could be adequate for the screen. Once potentially adequate libraries were generated, the extent of the mutagenesis could be assayed by checking for the presence of *can1* mutants. The *can1* gene encodes an arginine permease involved in the uptake of arginine and its analog canavanine. Canavanine is toxic to normal cells since it is incorporated in place of arginine, forming dysfunctional proteins. Cells with dysfunctional Can1 do not take in canavanine and survive. Similar to the selection of cells carrying a functional nutrient metabolism gene from an auxotrophic

strain, this provides a simple laboratory technique for mutant selection by growth media manipulation.

1.6 Characterization of screen parameters:

This aspect of the exploratory work involved determination of the growth and crossing conditions that would generate the maximum number of diploids. Refer to Figure 2 for a visual depiction of the fission yeast life cycle. In this work, mutant haploids are crossed to form diploids which are examined for normal sporulation behaviour (easily visualized under a microscope). The strains of haploids used in the mutant libraries each had a different adenine auxotroph genotype, so that when the alleles are combined in the diploid, by intragenic complementation at *ade6,* they are no longer auxotrophic (refer to Table 2 for genotypes of strains used in this work). This allows for the easy selection of diploids, and an assessment of diploid stability (in addition to microscopic examination) involving the isolation of spores by glusulase treatment.

1.7 Optimization of mutation location analysis:

This final stage of the work involved attempts at successful implementation of the integrant localization technique employed by Chua *et al.* (115). This technique involved the isolation of genomic DNA from cells identified as transformants by auxotrophic marker selection (*ura4*$^{+}$), digestion of the DNA by an enzyme that cuts frequently (less than every 4000 bp on average), but not within the marker/insert sequence, then circularization of the fragments for IPCR, and sequencing of the IPCR product for comparison with the fission yeast genome sequence to identify the insert location (potentially the gene of interest in the screen). Refer to Figure 3 for a pictorial depiction of this process.

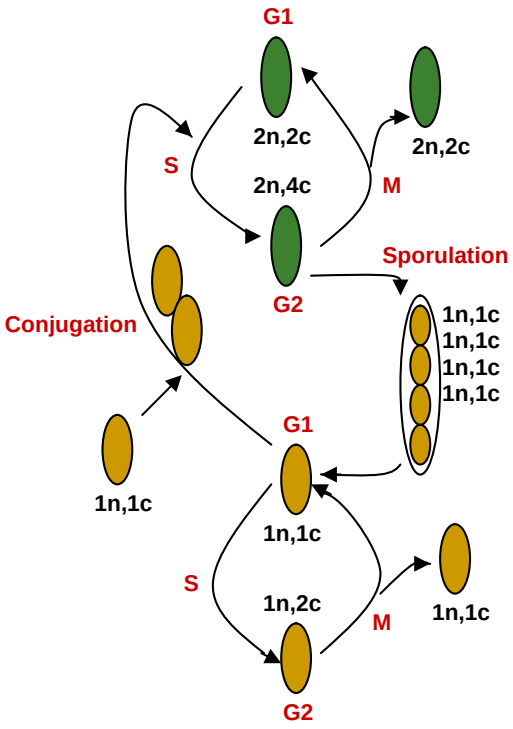

Figure 2: Fission yeast life cycle. Fission yeast normally propagate through the cell cycle in the haploid state (indicated in the lower portion of the diagram). Upon nutrient deprivation, they will conjugate or fuse to form diploids and propagate through this cell cycle (upper portion of the diagram), and then sporulate to from haploids again.

Table 2: List of fission yeast strains used in this work. All were from the pre-exising laboratory collection.

Strain	**Genotype**	**Mating type**
Sp2	*wt*	*h* $^{-}$
Sp3	*wt*	*h* $^{+}$
Sp30	*ade6-210 leu1-32 ura4-D18*	*h* $^{-}$
Sp31	*ade6-210 leu1-32 ura4-D18*	*h* $^{+}$
Sp372	*ade6-216 leu1-32 ura4-D18*	*h* $^{-}$
Sp661	*ade6-210 ura4-D18 rqh1::KMX*	*h* $^{-}$
Sp686	*ade6-210 leu1-32 ura4-D18 rad3::leu1*$^{+}$ *rqh1::KMX*	*h* $^{+}$
Sp693	*ade6-216 leu1-32 rqh1::KMX*	*h* $^{+}$
Sp705	*ade6-216 leu1-32 ura4-D18 rad3::leu1*$^{+}$ *rqh1::KMX*	*h* $^{-}$

1. Restriction Digest:

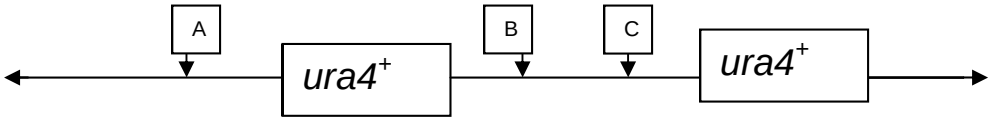

2. Ligation:

3. Inverse PCR:

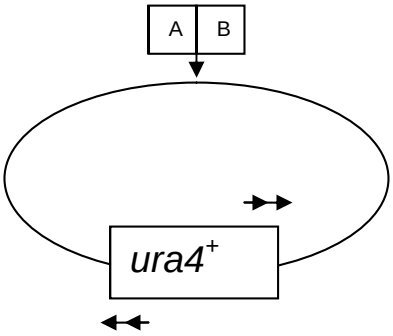

4. Sequencing:

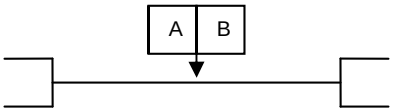

Figure 3: The process from Chua *et al.* (115) used to locate the insert in the mutant of interest, and thus, identify the disrupted gene targeted by the screen.
The process begins with the isolation of genomic DNA from haploid cells derived from the normally sporulating mutant. Genomic DNA is depicted in the top diagram by horizontal arrows, with the integrated sequence (*ura4*$^{+}$*)* shown in the middle. Genomic DNA is digested (indicated by letters with vertical arrows cutting into the horizontal genome). The next stage involves the ligation of the digested genomic DNA fragments. The stage of inverse PCR (IPCR) requires these fragments to be circularized, and utilizes primers that begin PCR at the ends of the *ura4*$^{+}$ insert sequence, which replicate in a direction moving away from the *ura4*$^{+}$ insert. The IPCR reaction was run once with the inner nested primers, and then again (using a sample of the first IPCR reaction) using a second set of primers to amplify the desired product. The double set of primers are indicated by horizontal arrows above and below the *ura4*$^{+}$ integrant. The IPCR product is a linear DNA fragment with the ends of the *ura4*$^{+}$ insert sequence at its ends. The interior of the fragment is now the genome sequence that once surrounded the randomly integrated *ura4*$^{+}$ fragment. This can be sequenced, allowing for the identification of the disrupted gene.

Chapter 2: Materials and Methods

2.1 Fission yeast strains and growth conditions:

Fission yeast strains used in these studies contained various nutrient deficiency, DNA damage, and replication checkpoint gene mutations and are listed and described in Table 2. Starter cultures for most procedures consisted of supplemented yeast extract medium (YES) in either liquid or plate form. Incubations were generally at 30 °C, with constant agitation of liquid media. Subsequent growth conditions consist of *S. pombe* minimal medium (PM) with nutrient and selective supplements as required, or sporulation medium (SPA) when crossing was desired.

YES consisted of 5 g/L yeast extract (Fisher Biotech, Nepean, ON), 30 g/L dextrose (Becton Dickinson, Oakville, ON) and 150 mg/L adenine (A), leucine (L), and uracil (U) (Bioshop Canada Inc., Burlington, Canada). PM consisted of 3 g/L phthalic acid (ICN Biomedicals Inc., Aurora, OH), 1.8 g/L Na_2HPO_4 (Bioshop), 20 g/L dextrose, and 5 g/L NH_4Cl (Bioshop), 20 ml/L of 50× PM Salts (0.26 M $MgCl_2$ (Fisher), 4.99 mM $CaCl_2$ (Fisher), 0.67 M KCL (Sigma, Oakville, ON), 14.1 mM Na_2SO_4 (Fisher)), 1 mL/L of 1000× PM vitamins (4.2 mM panthothenic acid (ICN), 81.2 mM nicotinic acid (Sigma), 55.5 mM inositol (ICN), 40.8 µM biotin (Bioshop)), and 100 µL of 10000× PM minerals (80.9 mM boric acid (ICN), 23.7 mM $MnSO_4$ (ICN), 13.9 mM $ZnSO_4$ (Fisher), 7.4 mM $FeCl_2$ (Fisher), 2.47 mM molybdic acid (ICN), 6.02 mM KI (Bioshop), 1.6 mM $CuSO_4$ (Fisher), 47.6 mM citric acid (Fisher)) were added, as well as 150 mg/L adenine, leucine and/or uracil as required for nutrient supplementation. For PM (canavanine) medium, 75 µg/mL canavanine sulfate (Calbiochem, San Diego, CA) was added to the PM media ingredients just listed. SPA consisted of 10 g/L dextrose, 1 g/L KH_2PO_4, 1 mL/L of 1000× PM vitamins, and 45 mg/L adenine, leucine and uracil.

Other alterations to basic media recipes were made as required for specific purposes and are mentioned elsewhere. These include the low dextrose (5 g/L) PMALU media in which strains were grown prior to lithium acetate transformation, and the PMAL canavanine medium on which strains were grown to select for *can1*$^{-}$ mutants.

2.2 Bacterial strain and growth conditions:

The EC 489 strain (One Shot TOP10 Competent Cells (F^{-} *mcr*A Δ(*mrr-hsd*RMS-*mcr*BC) f80*lac*ZΔM15 Δ*lac*X74 *rec*A1 *ara*D139 Δ(*ara-leu*)7697 *gal*U *gal*K *rps*L (Str^{R}) *end*A1 *nup*G) - Invitrogen Canada Inc., Burlington, ON) of *Escherichia coli* contained the *ura4*$^{+}$-carrying plasmid vector (pCR-BluntII-TOPO plasmid vector - Invitrogen Canada Inc., Burlington, ON). This strain was used to clone the *ura4*$^{+}$ fragment required for insertional mutagenesis of fission yeast strains. The bacterial strain was propagated in Luria-Bertani (LB) media, consisting of 10 g/L tryptone/peptone (Becton Dickenson), 10 g/L NaCl (Fisher), and 5 g/L yeast extract, supplemented with 50 µg/mL kanamycin sulfate (Bioshop) to select for only cells carrying the TOPO vector. The same ingredients were used to make LB plates, with the addition of 20 g/L agar. Plates were incubated at 37°C and liquid cultures were incubated at 37°C with constant agitation.

2.3 Transformation of fission yeast strains (insertional mutagenesis):

2.3.1 *ura4*$^{+}$ propagation:

The *ura4*$^{+}$ gene was in the DNA fragment used for random insertional mutagenesis of the fission yeast strains. The *ura4*$^{+}$ gene was propagated using the pCR-BluntII-TOPO plasmid vector in *E. coli*. The *E. coli* strain (EC489) was grown in 250 mL LB (50 µg/mL kanamycin sulfate) media overnight at 37°C and the plasmid DNA was harvested using the QIAprep Spin Miniprep kit (Qiagen Inc., Mississauga, ON) for the generation of the Sp705 and Sp686 (*rad3*^{0}*rqh1*^{0} fission yeast) mutant libraries and the cesium chloride –

ethidium bromide gradients method (117) for the generation of the Sp30 libraries. The cesium chloride method of DNA preparation involved the inoculation and overnight growth at 37°C of EC489 in 500 mL of LB (50 µg/mL kanamycin sulfate) media. The cell culture was then split in two and harvested by centrifugation at 6000 rpm (8 cm radius) for 15 min. Each pellet was resuspended in 6 mL of lysis buffer (50 mM glucose, 25 mM Tris-Cl pH 8.0, 10 mM EDTA pH 8.0) and placed in ice for 10 min before 12 mL of 0.2N NaOH/1%SDS was added and mixed by inversion. This mixture was then iced for a further 30 min before the addition of 9 mL 3M NaOAc pH 5.2 and mixed by inversion, then iced again for 30 min. The mixture was centrifuged at 10,000 rpm (8 cm radius) for 30 min and the supernatant was strained into another tube before adding an equal volume of isopropanol to the supernatant, mixed by inversion and incubated at room temperature for 1 h, then centrifuged at 3500 rpm (8 cm radius) for 30 min. The supernatant was then discarded and the pellets were dried slightly by inversion for 5 – 10 min. The pellet was then resuspended in 11 mL distilled water and 0.3 mL 10 mg/mL ethidium bromide was added before mixing and weighing. An equal weight of CsCl powder was then added and mixed before the liquid was put into Quick-Seal tubes (Beckman Coulter Canada Inc., Mississauga, ON) and centrifuged at 60,000 rpm (5 cm radius) for at least 16 h at 20°C. The Quick-Seal tube was then punctured using a 20G needle on a 3 mL syringe and the lower band was withdrawn. The ethidium bromide was removed by successive extractions with water saturated isoamyl alcohol (50:50) until the upper organic phase was colourless, and an equal volume of water was added. An equal volume of isopropanol was added to this final volume before it was mixed by shaking, and the resultant mixture was left to settle. Water (0.2 mL) was added and mixed until only one phase was apparent after settling. The solution was then divided into

microcentrifuge tubes and centrifuged at 13,000 rpm (8 cm radius) for 10 min. The supernatant was removed and the pellet was resuspended in 200 µL water before being left at room temperature for 1 h. The tubes were then combined into half the number and 1/10 volume of 3M NaOAc pH 5.2 was added, followed by 2.5 volumes of absolute ethanol and mixed by inversion. The mixture was centrifuged at 13,000 rpm (8 cm radius) for 10 min and washed twice in 70% ethanol. The pellet was dried by vacuum desiccation for 5 min and resuspended in 30 µL distilled water or TE. The purity and concentration of this DNA solution was then determined by spectrophotometry.

To remove the *ura4*$^+$ gene fragment from the plasmid vector, a restriction digest with the *Hin*dIII restriction enzyme (New England Biolabs Inc., Ipswich, MA) (recognition sites on either side of the *ura4*$^+$ gene) was run for 2 h at 37°C with 1 unit of enzyme per 1 µg of DNA. The reaction was then heat inactivated at 65°C for 20 min.

2.3.2 Transformation procedure:

The following conditions were those initially attempted in accordance with previously published work (115, 118), but variations were made to increase transformant yield, and are mentioned later: In preparation for the insertional mutagensis, fission yeast strains were first grown to saturation (30 - 60 × 10^7 cells/mL) in YES media, and then to mid-log phase (0.5 – 1 × 10^7 cells/mL) in 100 mL of PMALU (0.5 × glucose) media at 30°C. The mid-log cell culture was then pelleted by centrifugation at 3000 rpm (8 cm radius) for 5 min and washed once with distilled water and once with 0.1 M lithium acetate pH 4.9. The cells were resuspended in 0.1 M lithium acetate pH 4.9 at 1 × 10^9 cells/mL in 100 µL aliquots and incubated at 30°C for 1 h. Following this incubation, 1 µL of *ura4*$^+$ DNA in 15 µL TE was added to each aliquot of cells and again incubated for 1 h at 30°C. A 290 µL volume of PEG-3350 was added to each aliquot, and incubated for

1 h at 30°C. The cells were then heat shocked at 43°C for 15 min and allowed to recover at room temperature for 10 min before resuspension in 10 mL PMALU media and incubation at 30°C for 30 min with constant agitation, and at room temperature for 30 – 90 min without agitation. Transformants were then selected by plating onto PMAL (only those cells having integrated the *ura4*$^{+}$ gene survive in uracil deficient media). These plates were incubated for up to 2 weeks at 30°C to allow colonies to form.

2.3.3 Transformant/mutant libraries:

Plates containing transformants had colonies counted and mixed together in 20% glycerol, then stored in multiple microcentrifuge tubes at -80 °C. In determining the concentration of transformants in the library, and the extent of the mutagenesis, one tube was thawed and plated onto PMAL and PMAL (canavanine) plates in 10 × serial dilutions. From the number of colonies grown up on PMAL plates, the concentration of transformants in the library was determined, and the extent of the mutagenesis was quantified by the frequency of *can1* mutants in the library (calculated by dividing the number of colonies grown up on a PMAL (canavanine) plate by the number of colonies grown up on a PMAL plate).

2.4 Determination of conditions required for rad3^{0}rqh1^{0} transformant screen:

2.4.1 Screen for viable sporulating *rqh1*^{0}*/rqh1*^{0} diploids using spontaneous rate of mutagenesis:

A colony of each of the fission yeast strains Sp661 and Sp693 (Table 2) propagated on YES plates were grown overnight at 30°C in 10 mL YES (to 1×10^{6} - 1×10^{7} cells/mL), then 50 µL of each strain was mixed and plated on SPA media. The cross plates were incubated at 30°C for approximately 24 h, then removed and 1/10th of this cross was plated onto PM media and incubated at 30°C until colonies were clearly visible

and easily sampled (approximately 1 week). Samples of the resulting colonies were then examined under 40X magnification and 52 of the largest colonies with visibly sporulating diploids were sampled and spread again on PM plates, then incubated at 30°C for 1 week. A colony from each of these plates was again re-plated on PM and grown at 30°C for 3 days. A sample of each was then examined under 40X magnification and the percentage of sporulating cells was scored. Those showing greater than 50% sporulation were re-plated on YE and allowed to grow at 30°C until colonies were large enough to sample easily. A colony from each plate was spread onto PM to induce sporulation again, and grown for 2-3 days at 30 °C. A colony was then taken and mixed with 10 µL glusulase® in 1 mL distilled water and left at room temperature overnight (to kill vegetative cells, leaving only spores). These cells were then pelleted, washed twice with distilled water, and 10 × serial dilutions were plated on YES and grown at 30°C for 1 week. In order to determine adenine deficiency mutation type and mating type of each, six colonies were taken from each new strain (*rqh1*^{0}*/rqh1*^{0} mutants with normally sporulating diploids) and spotted (2 µL of each colony in 100 µL water) onto YE or SPA. The adenine deficiency type is clearly visible on YE in the varied red coloring of the colonies: the *ade6-216* type results in dark red colonies, whereas the *ade6-210* type results in light red colonies. The mating type was determined by crossing each new strain with Sp2 and Sp3 (Table 2) on SPA plates and examining cells for the presence of sporulating diploids after 2-3 days incubation at 30 °C. Once the adenine deficiency and mating type for each new strain was determined, they were crossed with their complementary *rqh1*^{0}*rad3*^{0} parental strains and *wt* strains on SPA as described for the previous crosses, then spread onto PMLU and colony growth compared to that of the *wt* × *wt* and *wt* × *rqh1*^{0}*rad3*^{0} strain crosses.

2.4.2 Procedure for optimal diploid yield of rqh1^{0}rad3^{0} cross:

Strains Sp372 and Sp686 (Table 2) were grown to saturation (30 - 60 $\times 10^7$ cells/mL) in YES media, and then to mid-log phase (0.5 – 1 $\times 10^7$ cells/mL) in YES at 30 °C. Volumes varied with the cell number required for each cross. Crosses of 1×10^6, 1×10^7 and 1×10^8 cells of each strain were set up by pelleting the required number of log phase cells, resuspending in 100 µL SPA media, mixing with the 100 µL suspension of the other strain to be crossed, and this 200 µL mixture was then plated onto SPA. Five different crosses of Sp372 × Sp686 and Sp705 × Sp686 for each of the cell quantities specified above were plated and incubated at 30°C for 12 h, 21 h, 26 h, 36 h, and 46 h, when at each time point the contents of one plate were removed into 1 mL of water and a 10 × dilution series was made. Each dilution (1/10 – 1/100,000) had 100 µL plated onto PMLU and plates were incubated at 30°C for 1 – 2 weeks when diploid colonies were counted.

2.5 Locating the insert in transformants:

The following conditions are those that resulted in an inverse PCR product:

2.5.1 Genomic DNA extraction:

This procedure was based on that used previously (115, 119), and was as follows: A sample of the transformants from the random mutagenesis library was grown on YES plates until colonies were visible (or PMAL (canavanine) plates when selecting *can1* mutants). Single colonies were selected and grown to saturation (30 – 60 × 10^7 cells/mL) in 100 mL YES. The media was divided into two 50 mL tubes and cells were pelleted by spinning at 3000 rpm (8 cm radius) for 5 min and the following treatment was applied to each half of the cells: resuspended in 5 mL 50 mM Citrate Phosphate pH 5.6, 40 mM EDTA, 1.2 M Sorbitol, then 2 mg Zymolyase-20T was added and incubated at 37°C for at least 60 min until most of cells appeared black under a phase contrast microscope after

the addition of 1 µL 10% SDS to 10 µL of cells. Cells were then resuspended in 15 mL 5 × TE, 1.5 mL 10% SDS was added and mixed, and the solution was incubated at 65°C for 5 min to turn all cells black under phase contrast microscopy examination. Lysed cells were incubated on ice for 30 min after the addition of 5 mL 5 M potassium acetate, then centrifuged at 5000 rpm (8 cm radius) for 15 min. The supernatant was then passed through gauze, followed by the addition of 20 mL ice cold isopropanol and incubated at – 20°C for 5 min. After centrifuging for 10 min at 1000 rpm (8 cm radius), the pellet was dried and resuspended in 3 mL 5 × TE with the addition of RNase to a final concentration of 20 µg/mL and incubated for 1 h at 37°C. Following the addition of 0.1 % SDS, and 20 µg/mL, cells were incubated at 65°C for 1 h. After this incubation, 3 mL phenol/chloroform (1:1) was added, mixed, centrifuged at 10,000 rpm (8 cm radius) for 10 min, then the upper phase was transferred to another tube followed by the addition of 3 mL 3 M sodium acetate and 7.5 mL ethanol, then mixed and incubated at – 20°C for at least 4 h. DNA was then pelleted, washed with 5 mL cold 70% ethanol, dried, and resuspended in TE.

2.5.2 Restriction Digest:

Isolated genomic DNA was phenol/chloroform purified and precipitated again with sodium acetate / ethanol if necessary to ensure the DNA was of high purity (assessed by a spectrophotometer 260/280 ratio of approximately 1.8). The digest was then set up for 8 h at 37°C with constant agitation in a 50 µL reaction of 4 – 8 µg DNA with 1 unit/µg of restriction enzyme *Hha*I. The reaction was then heat inactivated at 65°C for 20 min, and phenol/chloroform purified and sodium acetate / ethanol precipitated again.

2.5.3 Ligation:

Ligation/circularization of digested genomic DNA fragments was conducted as done previously (115) in a 20 µL reaction using 3 units T4 DNA Ligase (New England Biolabs Inc.) with 100 ng DNA and incubated for 16 h at 12 °C. This low DNA concentration favours intramolecular ligations. The reaction was then heat inactivated at 65°C for 20 min.

2.5.4 Inverse PCR:

Following the procedure of Chua *et al.* (115), the 20 µL ligation reactions were used directly in 100 µL PCR reactions with 60 pmols of each nested oligo primer (Table 3), 200 mM dNTPs, a final concentration of 2 mM $MgSO_4$ (provided in Taq DNA polymerase buffer), and 2.5 units Taq DNA polymerase (New England Biolabs Inc.). The PCR reactions were subjected to an initial 5 min heat denaturation step before the addition of Taq DNA polymerase, followed by 35 cycles of denaturation (95°C for 60 sec), primer annealing (55°C for 30 sec) and extension (70°C for 4 min). A second 100 µL PCR was then set up with a second set of oligo primers (within the new template sequence) (Table 3) using 2 µL of the previous PCR as template, and other conditions were as described for the previous reaction.

2.5.5 Gel electrophoresis:

Gel electrophoresis was used primarily to check if DNA was digested and to examine the Inverse PCR (IPCR) products, but was also used for DNA gel extractions to isolate IPCR product bands of particular sizes (as explained in the Results section). Gels were 1% agarose in TAE buffer, with bands visualized using ethidium bromide and UV

Table 3: Oligo primers used for Inverse PCR (IPCR) (from Chua *et al.* - 115). IPCR involved an initial reaction using nested primers ("first reaction") and a subsequent reaction to further amplify the desired product using primers ("second reaction") within the IPCR product of the first reaction.

IPCR	**Sequences** (5' to 3')	
	Forward	**Reverse**
First reaction	CAAAGTGCAAACATTATCATGAAAAAGAAC	GTGGAGTCTATGGAGCTGGTCGTAATCC
Second reaction	CACCATGCCAAAAATTACACAAGATAGAAT	TTTGGTTGGTTATTGAAAAAGTCGATGCCT

light. DNA gel extractions were either conducted using crystal violet or ethidium bromide and UV light to illuminate DNA bands. In both cases the DNA bands were not visible, but given previous knowledge of where the desired bands should be relative to marker bands, their location could be estimated for gel extraction. Gel extractions were conducted using the QIAquick Gel Extraction Kit (Qiagen).

2.5.6 DNA purification:

DNA was purified frequently during the preparation of DNA for the IPCR procedure. The QIAquick PCR Purification Kit (Qiagen) was occasionally used to purify DNA, but generally the phenol/chloroform method was used. This procedure consisted of adding TE to the DNA to bring the volume up to 400 – 500 µL, adding an equal volume of phenol/chloroform 1:1, vortexing for 30 - 45 sec and separating layers by centrifugation at 13,000 rpm (8 cm radius) for 1 min. The top layer containing DNA was separated into another tube and the bottom layer with white precipitate on top was discarded. This procedure was repeated. An equal volume of chloroform was then added to the fraction containing DNA, vortexed for 30 – 45 sec and centrifuged at 13,000 rpm (8 cm radius) for 1 min. The top layer containing DNA was again separated into another tube and this procedure was repeated. A 2.5 × volume of 95% ethanol / 0.15 M NaOAc was added to the remaining DNA solution and DNA was precipitated at – 20°C for at least 1 h. DNA was then pelleted by centrifugation at 13,000 rpm (8 cm radius) for 10 – 15 min, washed once with 70% ethanol, and the pellet was dried before being resuspended in TE, and the DNA concentration and purity was determined by spectrophotometry.

Chapter 3: Results

3.1 Fission yeast mutant libraries, crossing conditions, and mutation localization:

Libraries of mutants were generated in fission yeast strains by random integration of a DNA fragment containing the *ura4*$^{+}$ gene (115, 120). The conditions described in the Methods section were varied to improve transformant yield. Variations in cell number, *ura4*$^{+}$ fragment concentration, and incubation times that lead to successful transformations are described in the following sub-section. The *rqh1*^{0}*rad3*^{0} strains (Sp705 and Sp686 – Table 2) were mutated with the goal of generating a library of mutants that contained at least one mutant form of every gene in the fission yeast genome. The purpose of the genome-wide mutagenesis and screen was to knock out and identify genes that normally promote the generation of replication associated genomic instability. Specifically, the identification of genes that promote regression of replication forks to form the unstable "chicken-foot" structure, was desired (Figure 1).

As a control, the Sp30 strain (Table 2) was mutated with the intention of knocking out and identifying the location of the *can1* gene. Following the random mutagenesis, the number of successful transformants was determined by counting the number of colonies that grew up on PMAL plates (only transformants were not auxotrophic for uracil). The minimum number of transformants required for the screen was predicted to be 10,000, since this is the lowest number that might theoretically include a full genome coverage worth of mutants. This is based on the fact that the fission yeast genome contains approximately 5000 genes (4,824 protein encoding), with approximately half (57%) of the genome being protein-coding sequence(1). Since this predicted minimum number of transformants may not be enough in reality, several multiples of this one theoretical genome coverage would be required. Once a transformation resulted in at least 20,000

transformants, cells were removed from the plates into glycerol solution and frozen in 1 mL aliquots at -80 °C. To type the cell concentration in the frozen libraries, a sample was thawed and dilutions plated onto minimal selective media (PMAL), and minimal selective media with canavanine. Following incubation for 10 days at 30 °C, colonies were counted, and initial cell concentration, and the concentration of canavanine resistant cells, in the stock was calculated. The rate of mutagenesis was indicated by calculating the frequency of *can1* mutants in the libraries, with the logic that one *can1* mutant per 10,000 transformants would confirm the initial hypothesis of a 50% mutation rate. The properties of the libraries are summarized in Table 4 and in the subsections below.

The Sp30 library was used to attempt the methodology of Chua *et al.* (115) in determining the *ura4*$^{+}$ insert location. The procedure involved digestion, circularization, and inverse PCR (the oligo primers within the *ura4*$^{+}$ fragment), followed by sequencing of the PCR product to determine the mutation location. This finding of the location of the *can1* gene would be of interest, since it is uncertain at present. The procedure was, however, not successful and the location of *can1* was not determined.

The planned fate of the Sp686 and Sp705 libraries is more complex since these were to be crossed for the genomic instability screen. The process began with the crossing of these libraries to form diploids that were screened for the ability to sporulate normally (potential mutants of interest). These mutant strains were then back-crossed to the parental and wild type strains, with the expectation that new mutants of interest would cross like wild types. The inverse PCR process was then applied to determine the mutation location, and thus, identify the disrupted gene. As explained in Figure 1, the mutated gene identified in the screen would normally promote replication associated genomic instability. A thorough investigation of the conditions required to cross the

Table 4: Summary of fission yeast strain mutant libraries created.

Library Strain	**Transformant Number**	**Transformed Cell Concentration**	***can1*$^{-}$ Concentration**	***can1*$^{-}$ Frequency**
Sp 705	24,500 colonies	2.7×10^{8} cells/mL	9.4×10^{3} cells/mL	3.47×10^{-5}
Sp 686	50,000 colonies	1.22×10^{6} cells/mL	50 cells/mL	4.1×10^{-5}
Sp 30 (1)	18,000 colonies	1×10^{5} cells/mL	400 cells/mL	4×10^{-3}
Sp 30 (2)	24,000 colonies	1.1×10^{5} cells/mL	200 cells/mL	2×10^{-3}

Sp705 and Sp686 libraries are described in the following sub-sections, but were not implemented in an actual cross since the mutation localization technique did not work. These results are described in detail below.

3.1.1 Generation and analysis of mutant libraries:

In the generation of the Sp705 (*rqh1^{0}rad3^{0}*) library, the transformation procedure was as described in the Methods section with these variations: the cells were initially grown to 1.1×10^{7} cells/mL, the final incubation was 4 – 5 h with agitation at 30°C and the cells were plated onto 91 PMAL plates. The transformation resulted in 24,500 colonies after incubating plates for 2 weeks. Since this number of transformants included multiple theoretical genome coverages, it was considered a potentially adequate library and stored at - 80 °C. From sampling the library and growing on media, the transformant concentration was determined to be 2.7×10^{8} cells/mL and the number of *can1* mutants to be 9.4×10^{3} cells/mL of library with a frequency of 3.47×10^{-5} (number of *can1* mutant cells / number of transformant cells) (Table 4). This presence of *can1* mutants in the library suggests that the mutation rate is approximately 30% rather than the theoretically hypothesized rate of 50%. The logic behind this calculation is that one *can1* mutant per 10,000 transformants would indicate a mutation rate of approximately 50% (considering that half the genome is protein-coding), and the *can1* mutant frequency of this library indicates a ratio of approximately one *can1* mutant per 30,000 transformants, and thus, a mutation rate of 30%. This library may therefore be just adequate to use in the screen.

In the generation of the Sp686 (*rqh1^{0}rad3^{0}*) library, the transformation procedure was as described in the Methods section except that the cells were plated onto 33 PMAL plates. The transformation resulted in 100,000 colonies after incubating plates for 2 weeks. This transformation was also considered adequate and two libraries of 50,000

transformants were stored at - 80 °C. From sampling one of the libraries and growing on media, the transformant concentration was determined to be 1.2×10^6 cells/mL and the number of *can1* mutants to be 50 cells/mL of library with a frequency of 4.1×10^{-5} (number of *can1* mutant cells / number of transformant cells) (Table 4). This presence of *can1* mutants in the library suggests that the mutation rate is approximately 35% (approximately one *can1* mutant per 25,000 transformants, rather than the expected one mutant per 10,000 transformants, or a mutation rate of 50%). This library should therefore be adequate to use in the screen. With potentially adequate mutant libraries, it was possible to go on to determine the conditions required for the next stage of the screen (as described in the following sub-sections).

Two Sp30 strain mutant libraries were also generated. The first transformation procedure was as described in the Methods section except that 200 mL of cells were initially grown to 0.2×10^7 cells/mL, 10 µg of *ura4*$^+$ DNA was added to each 100 µL aliquot of cells, and cells were plated onto 45 PMAL plates. The transformation resulted in 18,000 colonies after incubating plates for 2 weeks. The library was stored at – 80 °C. On sampling one of the libraries and growing on media, the transformant concentration was determined to be 1×10^5 cells/mL and the number of *can1* mutants to be 400 cells/mL of library with a frequency of 4×10^{-3} (number of *can1* mutant cells / number of transformant cells) (Table 4). The second transformation procedure was also as described in the Methods section except that 500 mL of cells were initially grown to 1.1×10^7 cells/mL, and cells were plated onto 43 PMAL plates. The transformation resulted in 24,000 colonies after incubating plates for 2 weeks. The library was stored at – 80 °C. On sampling one of the libraries and growing on media, the transformant concentration was determined to be 1.1×10^5 cells/mL and the number of *can1* mutants to be 200 cells/mL

of library with a resultant frequency of 2×10^{-3} (number of *can1* mutant cells / number of transformant cells) (Table 4). The presence of the *can1* mutants indicate that the library is adequate to continue with the next stage and determine the location of the mutation, and thus, the location of the *can1* gene. However, as already stated, the procedure required to locate the mutation was not successful in this study.

3.1.2 Characterization of parameters for the diploid screen:

Following the generation of the *rqh1*^{0}*rad3*^{0} libraries, it was necessary to determine the procedure for the next stage: the screen for diploids with a normally sporulating phenotype.

Initially, the screen was attempted by crossing two *rqh1*^{0} mutant strains (Sp661 and Sp693 – Table 2) without the random mutagenesis procedure, to see if stable sporulating diploids could be generated from a spontaneous rate of mutagenesis. On crossing Sp661 and Sp693 as described in the Methods section, 1618 colonies resulted on minimal (PM) media. This media selects for diploids since haploids of this strain are adenine deficient. Following examination under phase contrast microscopy, 52 of the largest colonies with clearly sporulating diploids were sampled and re-plated. Samples of the colonies were again examined under phase contrast microscopy and those with greater than 50% sporulation were re-plated and treated with glucolase so as to isolate haploid spores. These new strains were then analysed for adenine deficiency and mating type and crossed with the relevant *rqh1*^{0}*rad3*^{0} and *wt* strains. This cross was based on the logic that new mutations of interest would nullify the detrimental effects of the *rqh1*^{0} mutation, and behave as wild types in a crossing situation. It was therefore predicted that a cross between a new mutant of interest and a wild type strain would result in more diploids than a cross with the parental *rqh1*^{0} strain (and the same yield as a *wt* × *wt* cross). The number

of diploid colonies resulting from these crosses (new strains × *wt* and new strains × *rqh1^{0}rad3^0*) was the same, and less than a *wt* × *wt* cross. This led to the conclusion that these new strains, although derived from sporulating diploids from the original cross, are not in fact new mutants of interest. A spontaneous rate of mutagenesis is not adequate to generate enough mutants to quickly screen millions of diploids, and the proposed random insertional mutagenesis is required (115). Through this crossing of *rqh1^{0}rad3^0* mutant libraries, it was determined that a similar back-crossing process would be required in the actual screen for sporulating diploids, to determine whether any sporulating diploids were actually novel mutants of interest.

Given that a large screen of diploids would be necessary to find the gene of interest, the next task was to determine the conditions for maximal diploid yield. Maximal diploid yield was necessary because at least 6.25×10^8 diploids had to be screened in order to allow for every mutant in each library to be crossed with every mutant from the other library. This extent of crossing was required so that diploids with disruptions in both copies of the same gene might be generated (25,000 × 25,000 different mutants crossed from each Sp686 and Sp705 mutant library).

Investigative crosses were *wt* × *wt*, *wt* × *rqh1^{0}rad3^0* and *rqh1^{0}rad3^0* × *rqh1^{0}rad3^0*. These were conducted to determine the conditions for optimal diploid yield, and predict the conditions required to screen a hypothetical 6.25×10^8 diploids from crossing the *rqh1^{0}rad3^0/rqh1^{0}rad3^0* mutant libraries. Initially, crosses were attempted in liquid SPA media (very low nutrient formula to induce crossing), and incubated at 30°C until harvesting crosses onto PMLU plates at 6 h, 12 h, 18 h, 24 h, 33 h, 36 h, 42 h, and 48 h time points. The crosses consisted of 1×10^6, 1×10^7, and 1×10^8 cells each of Sp31 × Sp372 (*wt* × *wt*), Sp31 × Sp705 (*wt* × *rqh1^{0}rad3^0*), Sp705 × Sp686 (*rqh1^{0}rad3^0* ×

rqh1^{0}*rad3*^{0}), and Sp372 × Sp686 (*wt* × *rqh1*^{0}*rad3*^{0}). PMLU plates were incubated at 30°C for 2 weeks and the resulting growth consisted of a primarily red background cover (indicative of adenine deficient haploid cells) with few white colonies (diploid). These diploid colonies were sampled and replated onto PMLU and did form colonies again after 2 weeks incubation at 30°C (confirming diploid genotype). However, due to the low number of diploids resulting from these crosses, the liquid SPA cross conditions were considered inadequate for the screen.

The next crosses were attempted on SPA plates with the same (as above) numbers of cells and time points of harvest onto PMLU. The result was a carpet of cells (indistinguishable colonies), so it was clear that a dilution series was necessary when plating the cross mixture onto PMLU. With this in mind, crosses of Sp372 × Sp686 (*wt* × *rqh1*^{0}*rad3*^{0}), and Sp705 × Sp686 (*rqh1*^{0}*rad3*^{0} × *rqh1*^{0}*rad3*^{0}) with 1×10^{6}, 1×10^{7}, and 1×10^{8} cells were plated on SPA and harvested onto PMLU in a 10× dilution series at 12 h, 21 h, 26 h, and 36 h time points. The optimal diploid yield (PMLU plate colony count) from the Sp705 × Sp686 (*rqh1*^{0}*rad3*^{0} × *rqh1*^{0}*rad3*^{0}) cross was generated by the 1×10^{8} cell cross after 21 h on SPA plates (Figure 4 and Table 5). From these results it was concluded that for optimal diploid yield in the actual screen, cells should be harvested onto PMLU plates after 21 h of crossing on SPA plates. Given that diploid harvest after 21 h of crossing led to optimal diploid yield, a comparison of diploid yield from various crosses harvested at 21 h was made (Figure 5). A cross of 1×10^{8} cells from each strain resulted in the best diploid yield. In order to calculate the actual number of diploids that could be generated from any particular cross conditions, the Sp372 × Sp686 (*wt* × *rqh1*^{0}*rad3*^{0}) cross results were considered the best indication of hypothetical diploid yield from crossing the mutant libraries. It was then determined that a total of 1.33×10^{7}

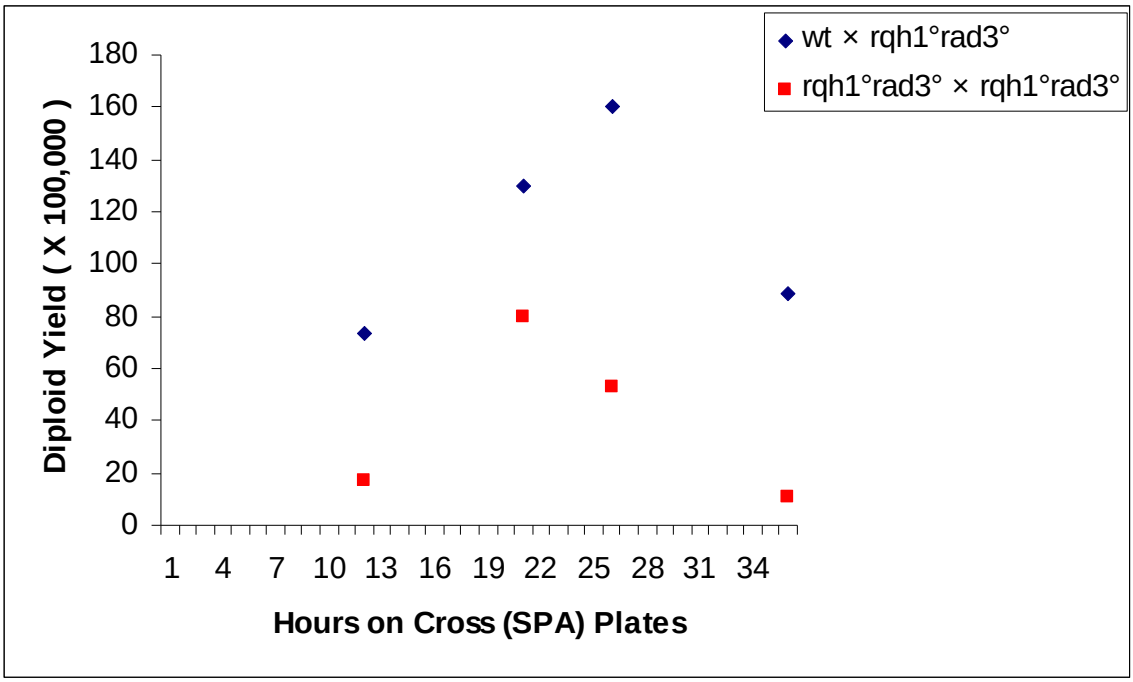

Figure 4: Diploid yield from crossing 1×10^8 cells of each strain (wt × rqh1^{0}rad3^0 and rqh1^{0}rad3^0 × rqh1^{0}rad3^0) for various periods of time.

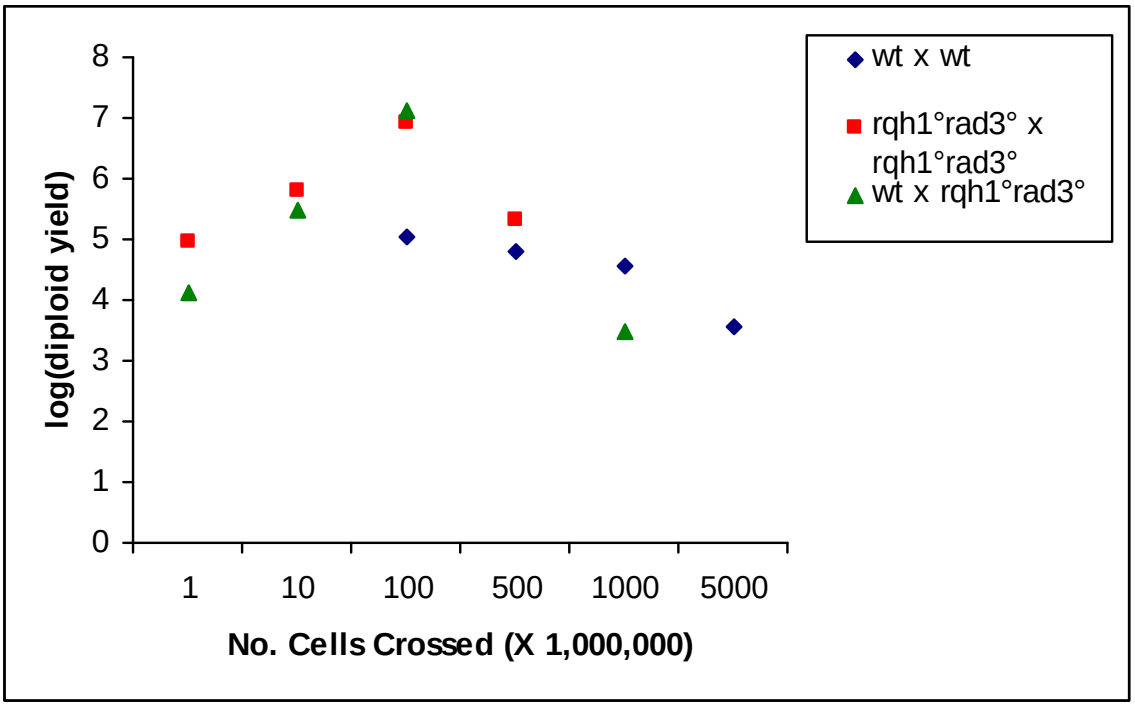

Figure 5: Logarithm (base 10) of diploid yield from crossing various numbers of cells of each strain (wt × wt, $rqh1^{0}rad3^{0}$ × $rqh1^{0}rad3^{0}$, and wt × $rqh1^{0}rad3^{0}$) for 21 h.

Table 5: Summary of diploid yield following various lengths of time crossing fission yeast strains as indicated.

Cross	Timepoint	Cells Crossed	Diploid Yield
wt×rqh1^{0}rad3^0	12 h	1×10^6 1×10^7 1×10^8	4.4×10^4 2×10^4 7.3×10^6
	21 h	1×10^6 1×10^7 1×10^8 1×10^9 5×10^9	1.3×10^4 2.8×10^5 1.3×10^7 3×10^3 3.2×10^7
	26 h	1×10^6 1×10^7 1×10^8	8.1×10^4 7×10^4 1.6×10^7
	36 h	1×10^6 1×10^7 1×10^8	7.2×10^4 8×10^4 8.9×10^6
rqh1^{0}rad3^0×rqh1^{0}rad3^0	12 h	1×10^6 1×10^7 1×10^8	6.4×10^4 4.2×10^5 1.7×10^6
	21 h	1×10^6 1×10^7 1×10^8 6×10^8	9.2×10^4 6.6×10^5 8×10^6 2×10^5
	26 h	1×10^6 1×10^7 1×10^8	2.8×10^4 6.9×10^5 5.3×10^6
	36 h	1×10^6 1×10^7 1×10^8	6.1×10^4 7.7×10^4 1×10^6
wt×wt	16 h	1×10^8	1.2×10^3
	18 h	1×10^8	4.6×10^5
	19 h	5×10^8	2.5×10^4
	20 h	1×10^8	2.7×10^5
	21 h	1×10^8 5×10^8 1×10^9 5×10^9	1.1×10^5 6.2×10^4 3.8×10^4 3.5×10^3
	24 h	1×10^8 5×10^8	1.8×10^5 3.1×10^4

diploids could have been harvested from this cross at 21 h. It would therefore be possible to screen a hypothetical 6.25×10^8 diploids in the actual screen if 48 crosses of 1×10^8 cells were made on SPA plates. The total number of cells that can be grown on a PMLU plate without too much background growth for diploid colonies to form is 1×10^8, and the total number of cells harvested onto PMLU plates after 21 h of a 1×10^8 cell cross was 6.7×10^8, meaning that a total of 322 PMLU plates would be required to harvest diploids in the actual screen (Table 6). It is also noteworthy at this point that the Sp705 × Sp686 (*rqh1*^{0}*rad3*^{0} × *rqh1*^{0}*rad3*^{0}) cross resulted in a diploid yield near equal to that of the Sp372 × Sp686 (*wt* × *rqh1*^{0}*rad3*^{0}), thus undermining a fundamental property of the screen: that *rqh1*^{0}/*rqh1*^{0} diploids are not stable without some additional phenotype altering mutation. This result further confirms the need for the additional screen stage of isolating spores from stable diploids, then crossing these new strains back to parental and wild type strains to observe crossing behaviour.

The experiments just summarized determined conditions that would work for the actual screen of 6.25×10^8 hypothetical diploids generated by crossing the mutant libraries. However, the number of crosses and plates required make it a difficult procedure, so other conditions to improve diploid yield were investigated. A full range of cell numbers and time points were attempted with various crosses, and these results confirmed the above rationale and plan for the screen (Table 5).

Given these results, it was concluded that the actual screen could be conducted by setting up 48 SPA plates with crosses of 1×10^8 cells from each of the Sp705 and Sp686 mutant libraries, and harvesting onto approximately 322 PMLU plates after 21 h of crossing. The number of PMLU plates required for diploid selection was determined as follows: The total number of cells (haploids and diploids) harvested from a 21 h 1 ×

Table 6: Conditions required to generate enough diploids to conduct the screen of 6.25×10^8 diploids. "Optimal Timepoint" indicates the hours of crossing found to generate the optimal diploid yield in investigative $rqh1^0rad3^0 \times rqh1^0rad3^0$ crosses. "Cell Number Crossed" is the number of cells of each strain to be crossed that resulted in the optimal diploid yield. "Diploid Yield of Each Cross" is the number of diploids generated from a 1×10^8 cell cross of wt × $rqh1^0rad3^0$ harvested at 21 hours. This number was then used to determine the "Cross Number Required" to generate 6.25×10^8 diploids to screen, and the "PM Plate No. Required" to harvest this many diploids is also indicated.

Optimal Timepoint	**Cell Number Crossed**	**Diploid Yield of Each Cross**	**Cross Number Required**	**PM Plate No. Required**
21 h	1×10^8	1.33×10^7	48 plates	320

10^8 cell cross on an SPA plate was 5×10^8 cells. This was then divided by the total number of cells that can be plated without generating excessive background cover (1×10^8). The result was then multiplied by the number of SPA plates required for the cross.

3.1.3 Optimization of mutation location analysis:

Following the crossing of the Sp705 and Sp686 mutant libraries, and screening for viable sporulating diploids, the next stage is to determine the location of the stability-causing mutation (indicated by "?" in Figure 1A). This procedure was attempted in order to ensure that it could be immediately implemented following the positive findings of the screen, and to verify the legitimacy of the mutant libraries.

The mutation localization procedure is based on the methodology of Chua *et al.* (115). It involves the isolation of genomic DNA from *ura4*$^+$ transformed cells, digestion of the DNA, ligation of the digested fragments to form circular pieces of DNA (at low DNA concentration to ensure that each DNA fragment is individually circularized), and Inverse PCR (IPCR). IPCR amplification starts from oligo primers within the inserted *ura4*$^+$ sequence, moving away from the insert around the circular fragment. The result is a linear fragment containing the DNA sequence from the original genomic DNA surrounding the *ura4*$^+$ insert, which when sequenced, can identify the mutated gene (Figure 3). The details of the procedure were varied until the successful method was developed, as described in the Methods section. Variations included: purification technique (phenol/chloroform extraction or PCR purification kits) and the resulting DNA purity (indicated by 260/280 ratio from spectrophotometer reading), digestion and ligation times and temperatures, and other variations mentioned below. Following each of the digestion and IPCR stages, the product was checked by running 2-5 µL in a 1% agarose electrophoresis gel. A complete digestion of genomic DNA was indicated by

distinguishable bands of various sizes among a smear of background DNA. The IPCR was considered successful if a single distinguishable band of at least 800 bp for the first IPCR and 550 bp for the second PCR was visible on the gel. These fragment lengths correspond to the expected (and observed) products of IPCR of just the circularized *ura4*$^+$ fragment, beginning at the nested primers for the first reaction, and at the outer primers for the second reaction. Examination of ligation products was also attempted by gel electrophoresis, but due to the small amount of DNA present, ligation products were not visible.

The insert localization procedure was initially attempted using Sp2 (*wt*) with the restriction enzyme *Eco*RI (New England Biolabs). This restriction enzyme's recognition site is located at either end of the *ura4*$^+$ gene, and a specific IPCR product of 5700 bp would confirm the success of the procedure. The ligation reaction was initially set up as suggested in the T4 DNA ligase instruction manual: 1 h at room temperature. The IPCR was first conducted using a relatively complex recipe for the amplification of large DNA fragments. The IPCR was set up in a 50 µL reaction using 0.5 µL *Pfx* polymerase (Invitrogen), "second reaction" oligos primers (Table 3), and other components as described in the methods section. The result of the initial IPCR (as visualized by gel electrophoresis) was three faint bands of approximately 1400 bp, 1100 bp, and 650 bp. Since these bands did not match the expected 5700 bp fragment, and the low DNA concentration with multiple bands did not lend itself well to sequencing, 2 µL of this reaction was used as the template for another PCR reaction using the same oligos primers with an additional 2 or 3 mM $MgSO_4$. The resultant band pattern from the PCR with 3 mM $MgSO_4$ was again faint, with one fragment of approximately 10,000 bp, and another of approximately 4,000 bp. These bands did not match that of the expected fragment.

Again, due to low concentration and multiple bands, they were not sequenced. The approximately 4000 bp fragment may however have been one part of the expected fragment, as the distance from one of the oligos primers to the nearest *Eco*RI site in the Sp2 strain sequence was almost 4000 bp long. If this is the case, it would suggest that the ligation reaction was not successful. Whatever the cause, this attempt at locating the insert was not successful, and the procedure was attempted again using Sp2 genomic DNA, but under different conditions. The procedure was now altered to follow more closely the model set up by Chua *et al.* (115). The ligation was for 16 h at 12 °C, and the IPCR recipe was altered to a 100 µL reaction with 2.5U of *Taq* polymerase, and the procedure consisted of a 5 min hot start at 95 °C, followed by 35 cycles of 95°C / 1 min; 55°C / 30 sec; 70°C / 4 min. The restriction digest was attempted using the enzyme *Hin*dIII, again giving a defined expected product, but of smaller size so as to increase the chance of it being amplified (*Hin*dIII sites are at either end of the *ura4*$^{+}$ gene). The only band to result from this IPCR was approximately 150 bp. This was too small to be the expected product and could not be sequenced.

A different source of genomic DNA was sought and a sample was taken from the already generated Sp705 mutant library and plated onto PMAL media. Four of the resultant colonies were sampled, genomic DNA was isolated, digested, ligated, and the IPCR reaction was set up using the same primer. This time, the restriction enzyme was *Hha*I as used by Chua *et al.* (115) because of its frequent recognition sites in the *S. pombe* genome. The product was again too small (approx. 150 bp) to be of interest. A second PCR was set up with 2 µL of the previous IPCR product as template, and run with the same oligo primers. The result was a smear of DNA on the electrophoresis gel. The next attempt was as above with samples of the Sp705 library again, but nested primers (“first

reaction" – Table 3) were now used for the first IPCR, which resulted in a smear of DNA on the electrophoresis gel. The second PCR was set up with the "second reaction" (Table 3) oligo primers and the result was similar multiple band patterns for each of the different DNA samples. This outcome was considered inadequate due to the multiple band pattern which could not be sequenced. Given that this unsuccessful outcome may be a result of the IPCR not working, it was reattempted with the addition of 2 mM $MgSO_4$ in the second PCR, and the repetition of the digest, ligation, and IPCR using tissue culture water (the pH of the distilled water used previously may have been affecting the process). These manipulations made no difference, with either no DNA or multiple bands appearing again on the electrophoresis gel after the IPCR reactions. During this process, it was also considered that the fact that restriction digests were conducted for 12-16 h initially, may have led to degradation of DNA. A 4 h digest was then attempted. This digest was however inadequate (as observed in undigested DNA on an electrophoresis gel). A restriction digest incubation of 8 h did result in a successful digestion of DNA and was considered optimal for these procedures.

With the lack of success using Sp2 and samples from the Sp705 mutant library, a sample of the first Sp30 mutant library was plated onto PMAL (canavanine) media. The selection of these specific transformants (*can1* mutants) meant that the success of this procedure would not only determine the protocol to apply in the screen, but would determine the location of the *can1* gene. In detail, the DNA was isolated and treated as described in the Methods section, using tissue culture water instead of the previously used Millipore double distilled water. The result of the first IPCR was a band of approximately 800 bp common to all samples, and the result of the second PCR was a band of approximately 550 bp (Figure 6). Since there were no other background bands present,

the result of the second PCR was sequenced. The result was a sequence that consisted of the two portions of the *ura4*$^+$ sequence between the outer primers and the *Hin*dIII recognition sites, joined at the *Hin*dIII sites, as would be expected if the *ura4*$^+$ fragment was ligated to itself to form a circular fragment that then underwent IPCR successfully. The difference in the size of the fragments seen after the first IPCR and the second PCR is accounted for in the difference in sequence between the two primers used (the nested primers used in the first reaction would result in a difference of approximately 250 bp over the product of the primers used in the second reaction). So although the ligation and IPCR procedure was successful, and the digests were confirmed by examination on an electrophoresis gel, the sequence surrounding the *ura4*$^+$ integrant was not determined. In regards to the goal of applying this insert localization technique to our mutant libraries, success was seen in the single *ura4*$^+$ based IPCR product that was indeed isolated from the mutant cells, and the details of this successful procedure are described in the Methods section. The procedure could not however be considered successful in terms of the goal of determining the *ura4*$^+$ insert location, due to the nature of fission yeast transformation products.

As will be explained in the discussion, it was thought that unintegrated *ura4*$^+$ fragments were providing the prominent template for IPCR. In an attempt to avoid this problem, DNA larger than the prominent 800 bp product of the initial IPCR was isolated by gel extraction, and served as the template for a second PCR amplification. In detail, more genomic DNA was required and the process was started again by sampling the Sp705 library onto PMAL (canavanine) plates. Six colonies were sampled and labeled A-F. Genomic DNA was isolated, digested, ligated, and the IPCR reactions were attempted

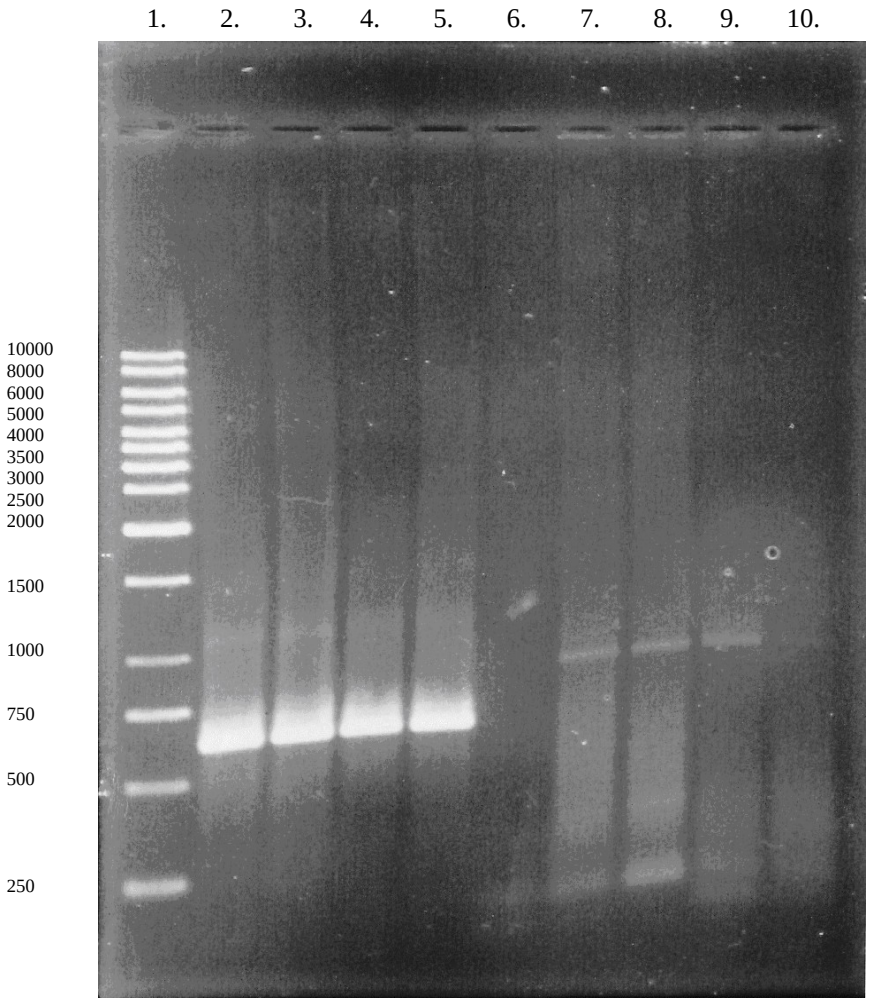

Figure 6: Ethidium bromide stained 1% agarose electrophoresis gel of IPCR products. Lane 1 contains 1Kb ladder (Fermentas GeneRuler), with band sizes indicated to the left of the image. Lanes 7-10 contain the result of the IPCR reaction of the digested and ligated DNA isolated from different colonies of *can1*$^{-}$ cells from the Sp30 mutant library, and lanes 2-5 contain the result of the second PCR reaction using 2 µL of the first IPCR result as template. The predominant fragment common to all of the first IPCR results is approximately 800 bp, and the predominant fragment in the second PCR result is approximately 550 bp, and the 250 bp difference in length between the fragments is accounted for by the difference in sequence included by the nested (first reaction) primers and the outer (second reaction) primers. The result of the second PCR was sequenced and corresponds to that expected of unintegrated *ura4*$^{+}$ fragments being successfully ligated and serving as the dominant template for IPCR.

several times with either 2 or 4 mM $MgSO_4$ in the second PCR. All of the samples resulted in IPCR products that were either too small in size, or had multiple bands, or bands were the same size as that already sequenced in the Sp30 library analysis (ie. representing unintegrated *ura4*$^+$ fragments). Sample B was of interest because it had the already sequenced band as well as another larger band. This larger band was potentially of interest as it may represent the desired IPCR product (containing sequence from the DNA region surrounding a successful *ura4*$^+$ insert). DNA gel extractions were then undertaken in an attempt to isolate DNA larger than the fragment already sequenced (800 bp after the first IPCR and 550 bp after the second PCR). In the first attempt, DNA from the first IPCR was run on a 1% agarose electrophoresis gel and stained with Crystal Violet. Since the DNA bands were still not visible, the distance from the well to the already sequenced band was estimated from the relative positions of the visible 1 kb ladder bands, and DNA above this point in each sample was isolated from the gel. From this DNA, the second PCR was then attempted with 100 ng of template DNA per reaction. The result was the same as before, with both the smaller already identified sequences (approximately 550 bp) and the larger band. It was therefore concluded that the gel extraction was not successful at removing the larger unknown band from the smaller known bands. The gel extraction was attempted again with Ethidium Bromide staining and UV illumination with the hope that the DNA bands might be more visible with this methodology. This was not however the case, and the location of DNA bands were again estimated using the relative location of the visible ladder bands, and the DNA above this point was extracted from the gel. The second PCR was run with both 10 ng or 100 ng DNA as template and with 2 or 4 mM $MgSO_4$. In all of these conditions, the result was a

smear of DNA on the post-PCR electrophoresis gel. With the impression that the UV light used in this most recent approach may have degraded the DNA, the Crystal Violet method was tried again, but with no success. The second PCR was run with various conditions as above and the result was again a smear of DNA on the electrophoresis gel. It was therefore concluded that gel extractions may not be an adequate addition to the IPCR procedure to identify the insert location. It is likely that some other method of insert localization, apart from PCR, will need to be implemented in this case.

Chapter 4: Discussion

The purpose of this work was to develop and implement a screen for genes, that in their normal function, can generate replication associated genomic instability in *S. pombe* (Figure 1). Work involved the application of previously developed techniques (115) to generate mutant libraries and locate the mutation site, and investigation of the conditions required for the screen. Mutant libraries were successfully generated, and a detailed protocol for the screen was developed. The technique employed to locate the generated mutations was not however successful. Given the various transformation products found in the mutant cells, this technique may not prove useful to the current screen. Due to this unpredicted challenge, the screen itself was not conducted, but the current work has developed the resources and protocol for the screen to be conducted upon identification of an adequate mutation localization technique.

4.1 Mutant Library Evaluation:

As described in previous sections, the lithium acetate transformation procedure was manipulated to generate as many transformants (mutants) as possible. In order to predict the adequate library size for this screen, the following logic was considered: the fission yeast genome has an average gene density of 0.56 with 4824 coding regions (1), and therefore, approximately 10,000 transformants would be required to have one theoretical genome coverage of mutants. However, it is thought unlikely that this theoretical estimate would actually be adequate to result in one mutant form of every gene. It was then proposed that at least double this estimate might provide an adequate library, so when libraries of 25,000 transformants in each strain were generated, they were considered potentially adequate libraries for the screen. A similar approach was applied in another study (Davidson *et al.* - 121) using this random mutagenesis technique

to screen for genes required for segregation of chromosomes in meiosis. In that study, only 1000 stable transformants were screened to identify 50 genes matching the criteria of their screen. The success of that study, where only 10% of the fission yeast genome was mutated (theoretically), confirms that our libraries, which ideally contain mutant forms of 100% of the genes in the fission yeast genome, should be adequate. In further support for the adequacy of our libraries, another similar study screened just 500 stable transformants to find 4 mutants of interest (Rodriquez-Gabriel *et al.* - 122).

Another finding of interest from Davidson *et al.* (121) was that most of the smaller colonies resulting from the transformation were not actually stable transformants. These colonies were found to contain unintegrated *ura4*$^{+}$ fragments that were still expressed as the *ura4*$^{+}$ phenotype. Davidson *et al.* (121) also went on to determine that about half of the large colonies (2-4 mm in diameter), were unstable transformants. Other previous work (Chua *et al.* - 115) found that 85% of transformants were unstable. Considering this literature in the generation of the current mutant libraries, colonies resulting from the transformation were categorized as small, medium, or large, where the large colonies would have approximately matched the categorization of Davidson *et al.* (121) (2-4 mm in diameter). Only medium and large colonies were considered in the count of transformants contributing to the current libraries. Considering these factors, and assuming that a similar frequency of unstable transformants (due to unintegrated extrachromosomal *ura4*$^{+}$ fragments) could be present in the current libraries, it is possible that only approximately 5000 of the transformants in each library are actually stable and of use to the screen. This number is not ideal, since at least 10,000 transformants would be required for one theoretical genome coverage of mutants. The libraries may however be adequate, given the success that other similar studies have had with just 1000 and 500

stable transformants (121 and 122, respectively), and the frequency of *can1* mutants discussed later. It is also possible to remove unstable transformants by growth on non-selective media for several generations (121). However, given the difficulty of testing thousands of transformants, it would be better to just attempt the screen with the current libraries. Also, given the nature of the screen, where only intrachromosomal *ura4*$^{+}$ fragments can cause a mutation that counteracts the *rqh1*^{0} instability, extrachromosomal *ura4*$^{+}$ fragments will not affect the response of cells to the screen conditions.

Once these mutant libraries in the *rqh1*^{0}*rad3*^{0} strains were generated, some measure of the extent of mutagenesis was required. A simple assay to evaluate library quality involves media containing canavanine, where only cells with a dysfunctional *can1* gene will grow. The *can1* gene encodes a plasma membrane arginine permease (123). Canavanine is structurally related to arginine, so cells mistake it for the amino acid and it is incorporated to form dysfuntional proteins (124). For this reason, cells with functional Can1 take in canavanine, which replaces arginine, resulting in cell death; whereas cells with dysfunctional *can1* do not take in canavanine and function normally. This assay provides an indication of mutagenesis rate, enabling inference as to the extent of mutagenesis in the library, based on a comparison of the number of *can1* mutants to the number of mutants generally (transformants selected for *ura4*$^{+}$ phenotype), referred to below as the *can1* mutant frequency.

When samples of the Sp686 and Sp705 (*rqh1*^{0}*rad3*^{0}) mutant libraries were thawed and plated, colonies did indeed grow on canavanine media, indicative of *can1* mutants. The calculation of *can1* mutant frequency in the libraries (*can1* mutant cells / transformed cells in the library) resulted in the data in Table 4. This suggests that approximately 4/100,000 library cells were *can1* mutants, which can be extrapolated to

suggest that the libraries of 25,000 transformants likely include one *can1* mutant. This calculation of *can1* mutant frequency is approximate, considering that it is using the number of transformed cells in the library, and the number of each transformant type varies with the size of colonies resulting from the lithium acetate transformation. The frequency of *can1* mutants in the libraries suggests a mutation rate of approximately 30%. This means that the initial guess that approximately 20,000 transformants might be adequate for the screen (double the 10,000 transformants required by theoretical prediction, reflecting a mutation rate of 50%), might be correct. The scope of the mutagenesis may therefore have been vast enough to provide an adequate basis for the screen in these libraries.

A consideration that may undermine this conclusion is the idea that the *can1* mutation may have arisen by spontaneous mutations during the propagation of cells at some point in the process, and may not have actually been caused by integration of the *ura4*$^{+}$ fragment at the *can1* site. This issue can be simply resolved by linkage analysis of the *ura4*$^{+}$ and *can1* phenotypes. This approach was attempted by crossing *can1* transformants from the library with wild type strains. The *ura4*$^{+}$ and *can1* phenotypes of the spores were analysed considering that if *ura4*$^{+}$ and *can1* are linked (and therefore may occupy the same locus), then the spores will display either both the *ura4*$^{+}$ and *can1* phenotypes, or neither, but not one without the other. Due to technical difficulties with media quality, no conclusions could be drawn, but it would be relatively easy to re-attempt this analysis. A similar approach was used by Ayoub *et al.* (125) to confirm genetic linkage of *ura4*$^{+}$ with the gene of interest to their screen which also used the methodology from Chua *et al.* (115).

4.2 Parameters for the Diploid Screen:

Considering the desire for mutant libraries containing at least one mutant form of every gene in the fission yeast genome, and the reasoning that the fission yeast genome contains approximately 5000 genes with approximately half the genome being protein-coding, it was thought that the libraries of 25,000 transformants would likely be adequate for this screen. Then, to screen diploids with two copies of the same mutation, for every gene in the genome, 6.25×10^8 (25,000 × 25,000) diploids had to be generated. It was therefore necessary to determine the crossing conditions that would result in the optimal diploid yield. Since the basis of the screen was the instability of *rqh1*^{0}*/rqh1*^{0} diploids, where at least one of the requisite haploids would theoretically contain a stability-generating mutation, it was expected that investigative crosses of *rqh1*^{0}*rad3*^{0} × *wt* would be most informative as to the number of diploids that could hypothetically be generated under any given cross conditions. Investigative crosses of *rqh1*^{0}*rad3*^{0} × *wt*, *rqh1*^{0}*rad3*^{0} × *rqh1*^{0}*rad3*^{0} and *wt* × *wt* were all conducted under various conditions to compare yield. Exact manipulations are described in the Results section. The diploid yield from crossing various numbers of cells for various periods of time was tabulated (Table 5). The optimal diploid yield resulted from 26 h of crossing 1×10^8 cells of *rqh1*^{0}*rad3*^{0} × *wt*. This *rqh1*^{0}*rad3*^{0} × *wt* cross was thought to be the best indicator of hypothetical diploid yield resulting from any given number of cells crossed in the actual screen. It was therefore concluded that 1×10^8 cells of each library could be crossed on one cross plate for optimal diploid yield. In determining optimal cross incubation time, *rqh1*^{0}*rad3*^{0} × *rqh1*^{0}*rad3*^{0} crosses are most important, since these are the strains used in the actual screen. Figure 4 was generated to compare the diploid yield after various cross incubation times for the *rqh1*^{0}*rad3*^{0} × *rqh1*^{0}*rad3*^{0} and *rqh1*^{0}*rad3*^{0} × *wt* crosses. In this Figure, it can

be seen that optimal diploid yield from the *rqh1^{0}rad3^0* × *rqh1^{0}rad3^0* cross was after 21 h. The optimal cross incubation time for the actual mutant library cross was thus predicted to be 21 h. Figure 5 was also generated to compare diploid yield after 21 h of crossing various cell numbers. Given these findings, the diploid yield from crossing 1×10^8 cells of *rqh1^{0}rad3^0* × *wt* for 21 h was considered the best indication of maximal diploid yield that might be screened in crossing the libraries. Considering that 6.25×10^8 diploids have to be screened, with a yield of 13.3×10^6 diploids from one cross plate, a total of 48 plates crossing 1×10^8 cells from each library would be required. Then given that a maximum of 1×10^8 cells (haploid and diploid) can go on one plate without having too much background growth, it was determined that the contents of the cross plates would need to be re-plated onto 320 diploid-selecting plates in the actual screen (Table 6).

Since the basis of the screen is the known instability of *rqh1^0/rqh1^0* diploids, an unexpected finding of these investigative crosses was the high diploid yield from the *rqh1^{0}rad3^0* × *rqh1^{0}rad3^0* crosses (Table 5, Figure 4 and 5). These results suggest that *rqh1^{0}rad3^0/ rqh1^{0}rad3^0* diploids are not as inherently unstable as expected, and an additional stage was added to the initial screen plan: Since simply selecting stable sporulating diploids will not likely be adequate to identify mutants of interest, the screen must also include the isolation of spores from stable (colonies showing greater than 50% sporulation after several re-platings) diploids, re-growth of these spores and observation of colony growth after back-crossing with parental and wild type strains. If these newly generated strains contain a mutation of interest, the effect of the *rqh1^0* mutation will be nullified and these strains will behave like wild types in a crossing situation. This additional screen stage was successfully implemented in an initial *rqh1^0* × *rqh1^0* cross. It determined that a spontaneous rate of mutagenesis with the *rqh1^0* mutation alone would

not be adequate for the screen, and is described in detail in the Results and Methods sections.

The unexpected high diploid yield from the *rqh1^{0}rad3^0* × *rqh1^{0}rad3^0* crosses might be explained by the following reasoning: the growth of diploid colonies would at least be partially dependent on the ability of cells to continue unhindered through the cell cycle, despite high levels of genomic aberration caused by the *rqh1^0* mutation. It is thus possible that the *rqh1^0* mutation alone with functional Rad3 would result in decreased cell growth and sporulation, because Rad3 would arrest the cell cycle in response to the aberrations caused by a lack of Rqh1 function. But cells lacking both Rqh1 and Rad3 would just continue to grow despite the highly compromised genome integrity. This finding may also suggest that if the screen as planned with *rqh1^{0}rad3^0* mutants is unsuccessful, it might be worth attempting with just *rqh1^0* mutants.

In summary, the following conclusion was drawn from the investigation of various cross conditions and the resultant diploid yield: The frozen mutant libraries must be thawed in YES media and incubated at 30°C until 4.9×10^9 (48 multiples of a 1×10^8 cell cross) cells of each strain are at mid-log phase growth. 1×10^8 cells of each strain then must be crossed on each of 48 SPA plates for 21 h. At this point, the crosses are to be harvested onto PMLU plates and incubated at 30°C for up to 2 weeks, or until colonies are clearly distinguishable. Any resultant stable diploids (colonies showing greater than 50% sporulation on PMLU plates after re-plating) should have spores isolated and grown to form new mutant strains which can be crossed back to parental and wild type strains to observe crossing behaviour. It should also be noted that the cell concentration of the mutant libraries was given in the results section. Thus, in sampling and thawing the libraries to conduct the screen, it can be ensured that the library sample is of an adequate

volume to contain at least one cell of each of the 25,000 transformants to be amplified by growth in rich media.

4.3 Mutation Location Analysis:

In the detailed preparation for the screen, it was necessary to ensure that the mutation localization procedure taken from Chua *et al.* (115) could be replicated successfully. Many conditions and DNA sources were varied until the successful procedure described in the methods section was developed. The procedure was perfected in the localization of mutations in a selection of *can1*$^{-}$ transformants from the first Sp30 library. The fragment amplified by IPCR was sequenced and found to be from the *ura4*$^{+}$ fragment, which was circularized and then amplified from the outward pointing primers, through the ends of the original linear fragment and back to the primers on the other side of the *ura4* sequence. This result could be explained by the finding of Davidson *et al.* (121), which determined that many of the apparently transformed cells contained unintegrated *ura4*$^{+}$ fragments. These fragments were still expressed as intrachromosomal DNA. It seems likely that in the current study, many of the transformants contain both integrated *ura4*$^{+}$ fragments (causing the *can1* disruption) as well as unintegrated *ura4*$^{+}$ fragments. On extraction of DNA from the *can1* mutant transformants, the extrachromosomal *ura4*$^{+}$ fragments were likely much more abundant and formed smaller PCR templates than intrachromosomal *ura4*$^{+}$. This would be because the latter templates contained not just the *ura4*$^{+}$ fragment, but also an area of genomic DNA surrounding the insert. Given this relative abundance (Chua *et al.* (115) found multiple copies of extrachromosomal *ura4*$^{+}$ in transformants), and smaller size of the unintegrated *ura4*$^{+}$ fragments, these would provide the preferred template for IPCR (126). This would

explain why only these fragments were amplified when the procedure was applied to *can1*$^{-}$ mutants from the Sp30 library.

In considering factors that might have resulted in the inability of this technique to locate the insert sites in the mutant libraries, completion of each individual stage in the process was checked. The quality of genomic DNA could be measured via spectrophotometry for purity and quantity, and by electrophoresis gel to ensure that DNA was not degraded (intact genomic DNA would appear as a bright band in the well, while degraded DNA would appear as a smear of multiple bands in the gel lane). The completion of digestion could be confirmed by the presence of multiple bands on an electrophoresis gel, and IPCR products were easily visualized on electrophoresis gel. The only stage that could not be tested readily was the ligation. Due to the small quantity of DNA present, and the specificity of this mixture as the template for IPCR, it could not be visualized on an electrophoresis gel. The presence of an IPCR product would suggest that the ligation must have worked. But, since this product was amplified from extrachromosomal *ura4*$^{+}$ fragments, these fragments may have circularized independently in the cell, prior to the extraction of DNA for this process.

In order to confirm the success of ligation, the conditions used in this work were compared to those found successful in other studies, using the formulae discussed below. Previous work recorded the percent circularization of DNA fragments resulting from various ligation conditions. Collins and Weissman (1984) (127) studied the effect of DNA fragment concentration on the percent circularization of single fragments. They found that a plot of ligation concentration (x-axis) against percent circles (y-axis) formed a reverse S-curve, demonstrating the quick decline in the proportion of DNA fragments circularized as the concentration of DNA increases. Their findings also fit with the model

proposed by Jacobson and Stockmayer (1950) (as cited in 127) where formulae were generated to calculate the percentage of DNA fragments that could be expected to circularize given any DNA fragment length and concentration. These formulae are shown below, where "j" represents the effective concentration of one end of a DNA fragment in the neighbourhood of the other end, "kb" represents the length of the fragment, and "i" represents the DNA concentration:

$$j = \frac{63.4}{(kb)^{1/2}} \ \mu g/ml$$

Then, given "j" and "i", the expected percentage of circles can be calculated:

$$\% \text{ circles} = \frac{j}{i + j} \times 100$$

Given these formulae, and the graph described above (127), the desires for optimal circularization frequency and adequate DNA concentration for IPCR, can be balanced mathematically. To illustrate with figures from the current study: The DNA is digested with the restriction enzyme *Hha*I, which generally cuts every 500-1000 bp in the fission yeast genome. The following ligation would circularize the desired fragments of approximately 2200 bp (1700 bp *ura4*$^+$ fragment + 500 bp of DNA surrounding insert). Considering the formulae stated above, the percent circles resulting from the ligation can then be calculated, given the DNA concentration of 5 µg/mL required for IPCR. Inserting these values for fragment length and DNA concentration into the formulae above, results in an expectation of 89.6% circles from the ligation conditions used in the current work. Lowering the DNA concentration would increase the percentage of fragments circularized, but would result in an inadequate amount of template DNA for IPCR. Given these constraints, 89.6% can be considered adequate for the current work. Thus, the

ligation was most likely successful, especially since the ligation conditions are the same as those successfully employed by Chua *et al.* (115).

Despite the fact that the insert localization technique from Chua *et al.* (115) could be successfully replicated, it may not work to locate the integrant in the current screen. This is due to the fact that extrachromosomal *ura4*$^+$ fragments remain in the transformed cells and serve as the prominent PCR template. It is likely that following the crossing of the mutant libraries, the resulting stable diploids with successfully integrated *ura4*$^+$, also contain unintegrated *ura4*$^+$ fragments that inhibit IPCR amplification of the desired fragment. Thus, this method will not be useful to identify the disrupted gene. A similar lack of success was seen in an attempt to apply this technique to locate mutation sites following similar screens (121, 122, 125). The latter found that 2 of the 4 mutant strains of interest were refractory to IPCR analysis. In trying to resolve their difficulty in implementing this technique, Davidson *et al.* (121) engaged in correspondence with many members of the fission yeast research community. They found that others had similar difficulties, and that alternative approaches were necessary. The lack of success may largely be due to the predominance of extrachromosomal *ura4*$^+$ fragments following electroporation and lithium acetate transformation of fission yeast, as found by Davidson *et al.* (121).

In the current investigation, a possible solution to this problem was attempted: Between IPCR reactions, the PCR product representing unintegrated *ura4*$^+$ fragments was removed (along with all smaller fragments) by gel extraction, to leave only larger template fragments. This allowed for any templates containing sequence around intrachromosomal *ura4*$^+$ integrants to be amplified in the second PCR. Most likely due to

the small amounts of DNA dealt with in this approach, and the inability to visualize DNA bands on a gel, this gel extraction method was not successful.

Other manipulations of the technique employed in this work may help to negate the influence of extrachromosomal *ura4*$^+$ as the predominant template for IPCR. It may also be possible to grow the transformants on nonselective media for several generations either before freezing into mutant libraries, or after thawing, but before genomic DNA isolation. The purpose of this would be to undermine the selective benefit of the extrachromosomal *ura4*$^+$ fragments to the cells, with the hope that these fragments will be expelled from the cells, or at least become insignificant relative to the number of cells with only intrachromosomal *ura4*$^+$. Thus, no longer providing the prominent *ura4*$^+$ sequence template for IPCR. After growth on non-selective media, successful transformants can be identified by sensitivity to 5-FOA (115, 120).

Another approach that might be attempted in the future, without physically removing the undesired extrachromosomal *ura4*$^+$ template, might be to manipulate PCR conditions so as to selectively amplify only larger template fragments. Dai *et al.* (126) extensively studied the PCR-suppression effect and the various PCR conditions that can be manipulated to selectively amplify larger or smaller fragments. The PCR-suppression effect involves the suppression of amplification of DNA molecules flanked by inverted terminal repeats. This is caused by the formation of “panhandle-like” structures as a result of the terminal repeat sequences annealing to each other. This structure prevents primer binding to the template, preventing amplification. Shorter DNA fragments are suppressed more easily than longer ones because they form the “panhandle” structure more easily (128). It is therefore likely that the shorter DNA template, that we do not want to amplify in the current work, can be suppressed by the addition of inverted repeats at the end of the

ura4$^+$ fragment. Then, following the detailed work of Dai *et al.* (126), the smaller undesired template could be selected against. Specifically, Dai *et al.* (126) concluded that since shorter templates form the "panhandle" structure more easily, conditions that increase the likelihood of inverted terminal repeat self-annealing would suppress the amplification of shorter template fragments. These conditions include: lower primer concentration to decrease competition between primer-template annealing and self-annealing; longer inverted terminal repeats to increase their melting temperature, so that self-annealing begins earlier than primer-template annealing when the reaction temperature decreases just prior to annealing, decreasing the chance of primer-template binding; and a lower annealing temperature since the "panhandle" structure is more stable than relaxed structures at these temperatures.

Although the most likely explanation for the failure to identify the mutation site is the presence of extrachromosomal *ura4*$^+$ fragments, there are other factors that might be considered. It might be useful to attempt the procedure with more than one restriction enzyme in future work. The enzyme applied with the most success in the current work, *Hha*I, has recognition sites that occur frequently within the fission yeast genome, often with a site or two within any given 1000 bp stretch of DNA. However, there are occasionally stretches of a few thousand base pairs without a *Hha*I restriction site. If the intrachromosomal *ura4*$^+$ fragment happened to be within one of these longer stretches, the IPCR might not successfully amplify this area of DNA surrounding the insert if it was more than 4000 bp long, since the extension time in the IPCR recipe was 4 mins. Although, as already stated from the IPCR results and the findings of others, the critical fault in the procedure is the prominence of extrachromosomal *ura4*$^+$ fragments.

Prior to attempting the actual screen (crossing the mutant libraries) it will be necessary to either manipulate the current approach for success, or apply some other mutation localization technique. Possible other approaches include: linkage analysis by crossing the transformed strains with strains containing different nutrient deficiencies. This approach was successfully implemented by Davidson *et al*. (121). In that work, a mutant transformant of interest (auxotrophic for histidine, but prototrophic for uracil due to the *ura4*$^{+}$ transgene) was crossed with another strain of opposite nutrient deficiency mutations. The spores were then analysed for segregation patterns of the various markers, finding that the *ura4*$^{+}$ integration (and therefore, the disrupted gene) was within 0.5 cM of the *his3* locus on Chromosome II. In the same study, another transformant was analysed using a similar approach, and finding that 24% of the *ura4*$^{+}$ colonies were mating type h^{+}, it was concluded that the *ura4*$^{+}$ transgene was approximately 33 cM from the mating type locus *mat1* on Chromosome II. The markers used in the previous study (121) are just two examples of the many possibilities available for further analysis in the current work.

4.4 Conclusion:

Libraries of mutants in both mating types of the *rqh1*^{0}*rad3*^{0} mutant strains were successfully generated. Considering the frequency of *can1* mutants in the libraries, and the success that similar screens have seen with far less extensive mutant libraries, the mutant libraries are likely adequate to employ in the currently planned screen. Ideal libraries for the screen would contain a mutant form of every gene in the fission yeast genome. Since this ideal would be very difficult to achieve, it is worth attempting the screen with the current (very extensive) libraries. The goal of the screen is then to cross the libraries so that diploids can be generated that contain two alleles of the same mutant gene of interest (Figure 1), overcoming the inherent instability of the *rqh1*^{0}*rad3*^{0} mutant

strains. In order to cross enough mutants to screen such a number of diploids, a large scale operation is required. The details of this complex screen were investigated and thoroughly mapped-out in the current work. Investigation of the details of the final stage in the process, the localization of the mutant of interest identified in the screen, proved unsuccessful. The technique adopted from Chua *et al.* (115) may not work in the current context, due to the presence of extrachromosomal *ura4*$^{+}$ fragments providing the predominant template for IPCR. Other manipulations, such as growing transformants on non-selective media for several generations to remove unstable transformants, and the manipulation of the IPCR to select for the larger intrachromosomal *ura4*$^{+}$ templates, should be attempted before completely discarding this approach. Alternative approaches are also outlined above and should be proven successful before the actual screen is attempted in future work.

References

1. Wood, V., Gwilliam, R., Rajandream, M.-A., *et al.* (2002) The genome sequence of *Schizosaccharomyces pombe*. *Nature* **415**: 871-880.
2. Forsburg, S. L. (1999) The best yeast? *Trends Genet* **15**: 340-344.
3. Elledge, S. J. (1996) Cell cycle checkpoints: preventing an identity crisis. *Science* **274**: 1664-1672.
4. Caspari, T., and Carr, A. M. (1999) DNA structure checkpoint pathways in *Schizosaccharomyces pombe*. *Biochimie* **81**: 173-181.
5. Humphrey, T. (2000) DNA damage and cell cycle control in *Schizosaccharomyces pombe*. *Mutation Research* **451**: 211-226.
6. Fearon, E. R., and Vogelstein, B. (1990) A genetic model for colorectal tumorigenesis. *Cell* **61**: 759-767
7. Loeb, L. A. (1991) Mutator phenotype may be required for multistage carcinogenesis. *Cancer Research.* **51**: 3075-3079.
8. Loeb, L. A., and Christians, F. C. (1996) Multiple mutations in human cancers. *Mutation Research* **350**: 279-286.
9. Ionov, Y., Peinado, M. A., Malkhosyan, S., *et al.* (1993) Ubiquitous somatic mutations in simple repeated sequences reveal a new mechanism for colonic carcinogenesis. *Nature* **363**: 558-561.
10. Loeb, L. A. (1991) Mutator phenotype may be required for multistage carcinogenesis. *Cancer Research* **51**: 3075-3079.
11. Loeb, L. A., Loeb, K. R., and Anderson, J. P. (2003) Multiple mutations and cancer. *PNAS* **100**: 776-781.
12. Bielas, J. H., and Loeb, L. A. (2005) Mutator phenotype in cancer: timing and perspectives. *Environmental and Molecular Mutagenesis* **45**: 206-213.
13. Venkatesan, R. N., Bielas, J. H., and Loeb, L. A. (2006) Generation of mutator mutants during carcinogenesis. *DNA Repair* **5**: 294-302.
14. Loeb, L. A. (2001) A mutator phenotype in cancer. *Cancer Research* **61**: 3230-3239.
15. Tomlinson, I., and Bodmer, W. (1999) Selection, the mutation rate and cancer: ensuring that the tail does not wag the dog. *Nat Med* **5**: 11-12.
16. Cairns, J. (1975) Mutation selection and the natural history of cancer. *Nature* **255**: 197-200.
17. Tomlinson, I. P., Sasieni, P., and Bodmer, W. (2002) How many mutations in cancer? *Am J Pathol* **100**: 755-758
18. Loeb, K. R., and Loeb, L. A. (2000) Significance of multiple mutations in cancer. *Carcinogenesis* **21**: 379-385.
19. Kinzler, K. W., and Vogelstein, B. (1997) Gatekeepers and caretakers. *Nature* **386**: 761-763.
20. Bellacosa, A. (2003) Genetic hits and mutation rate in colorectal tumorigenesis: versatility of knudson's theory and implications for cancer prevention. *Genes, Chromosomes & Cancer* **38**: 382-388.
21. Wang, X., Wang, L., Callister, M. D., *et al.* (2001) Human Rad17 is phosphorylated upon DNA damage and also overexpressed in primary non-small cell lung cancer tissues. *Cancer Research* **61**: 7417-7421.

22. Kataoka, A., Sadanaga, N., Mimori, K., *et al.* (2001) Overexpression of HRad17 mRNA in human breast cancer: correlation with lymph node metastisis. *Clin Cancer Res* **7**: 2815-2820.
23. Futreal, P. A., Liu, Q., Shattuck-Eidens, D., *et al.* (1994) BRCA1 mutations in primary breast and ovarian carcinomas. *Science* **266**: 120-122.
24. Miki, Y., Swensen, P., Shattuck-Eidens, D., *et al.* (1994) A strong candidate for the breast and ovarian cancer susceptibility gene BRCA1. *Science* **266**: 66-71.
25. Wang, C., Horiuchi, A., Imai, T., *et al.* (2004) Expression of BRCA1 protein in benign, borderline, and malignant epithelial ovarian neoplasms and its relationship to methylation and allelic loss of the BRCA1 gene. *J Pathol* **202**: 215-223.
26. Wooster, R., Neuhausen, S. L., Mangion, J., *et al.* (1994) Localization of a breast cancer susceptibility gene, BRCA2, to chromosome 13q12-13. *Science* **265**: 2088-2090.
27. Lee, S. B., Kim, S. H., Bell, D. W., *et al.* (2001) Destabilization of CHK2 by a missense mutation associated with Li-Fraumeni Syndrome. *Cancer Research* **61**: 8062-8067.
28. Bell, D. W., Varley, J. M., Szydlo, T. E., *et al.* (1999) Heterozygous germ line hCHK2 mutations in Li-Fraumeni syndrome. *Science* **286**: 2528-2531.
29. Gumy-Pause, F., Wacker, P., and Sappino, A.-P. (2004) ATM gene and lymphoid malignancies. *Leukemia* **18**: 238-242.
30. Savitsky, K., Bar-Shira, A., Gilad, S., *et al.* (1995) A single ataxia telangiectasia gene with a product similar to PI-3 kinase. *Science* **268**: 1749-1753.
31. Sancar, A., Lindsey-Boltz, L. A., Unsal-Kaccmaz, K., *et al.* (2004) Molecular mechanisms of mammalian DNA repair and the DNA damage checkpoints. Annu Rev Biochem **73**: 39-85.
32. Rotman, G., and Shiloh, Y. (1998) ATM: from gene to function. *Hum Mol Genet* **7**: 1555-1563.
33. Levine, A. J. (1997) p53, the cellular gatekeeper for growth and division. *Cell* **88**: 323-331.
34. Hollstein, M., Rice, K., Greenblatt, M. S., *et al.* (1994) Database of p53 gene somatic mutations in human tumors and cell lines. *Nucl Acids Res* **22**: 3551-3555.
35. Cleaver, J. (1969) Xeroderma pigmentosum: a human disease in which an initial stage of DNA repair is defective. *PNAS* **63**: 428-435.
36. Bronner, C. E., Baker, S. M., Morrison, P. T., *et al.* (1994) Mutation in the DNA mismatch repair gene homologue hMLH1 is associated with hereditary non-polyposis colon cancer. *Nature* **368**: 258-261.
37. Fishel, R., Lescoe, M. K., Rao, M. R., *et al.* (1993) The human mutator gene homolog MSH2 and its association with hereditary nonpolyposis colon cancer. *Cell* **75**: 1027-1038.
38. Liu, B., Nicolaides, N. C., Markowitz, S., *et al.* (1995) Mismatch repair gene defects in sporadic colorectal cancers with microsatellite instability. *Nat Genet* **9**: 48-55.
39. Moslein, G., Tester, D. J., Lindor, N. M., *et al.* (1996) Microsatellite instability and mutation analysis of hMSH2 and hMLH1 in patients with sporadic, familial, and hereditary colorectal cancer. *Hum Mol Genet* **5**: 1245-1252.
40. Kinzler, K. W., and Vogelstein, B. (1996) Lessons from hereditary colorectal cancer. *Cell* **87**: 159-170.

41. Futreal, P. A., Coin, L., Marshall, M., *et al.* (2004) A census of human cancer genes. *Nat Rev Cancer* **4**: 117-183.
42. Luzzatto, L. (2001) The mechanisms of neoplastic transformation. *European Journal of Cancer* **37**: S114-S117.
43. Hartwell, L. H., and Weinert, T. A. (1989) Checkpoints: controls that ensure the order of cell cycle events. *Science* **246**: 629-634.
44. Sancar, A., Lindsey-Boltz, L. A., Unsal-Kacmaz, K., *et al.* (2004) Molecular mechanisms of mammalian DNA repair and the DNA damage checkpoints. *Annu Rev Biochem* **73**: 39-85.
45. Zhou, B.-B. S., and Elledge, S. J. (2000) The DNA damage response: putting checkpoints in perspective. *Nature* **408**: 433-439.
46. Helt, C. E., Wang, W., Keng, P. C., *et al.* (2005) Evidence that DNA damage detection machinery participates in DNA repair. *Cell Cycle* **4**: 529-532.
47. Wang, W., Brandt, P., Rossi, M. L., *et al.* (2004) The human Rad9-Rad1-Hus1 checkpoint complex stimulates flap endonuclease 1. *PNAS* **101**: 16762-16767.
48. Smirnova, E., Toueille, M., Markkanen, E., *et al.* (2005) The human checkpoint sensor and alternative DNA clamp Rad9-Rad1-Hus1 modulates the activity of DNA ligase I, a component of the long-patch base excision repair machinery. *Biochem J* **389**: 13-17.
49. Toueille, M., El-Andaloussi, N., Frouin, I., *et al.* (2004) The human Rad9/Rad1/Hus1 damage sensor clamp interacts with DNA polymerase ß and increases its DNA substrate utilization efficiency: implications for DNA repair. *Nucleic Acids Research* **32**: 3316-3324.
50. Ritchie, K. B., Mallory, J. C., and Petes, T. D. (1999) Interactions of TLC1 (which encodes the RNA subunit of telomerase), TEL1, and MEC1 in regulating telomere length in yeast *Saccharomyces cerevisiae*. *Molecular and Cellular Biology* **19**: 6065-6075.
51. Xu, Y., and Baltimore, D. (1996) Dual roles of ATM in the cellular response to radiation and in cell growth control. *Genes and Development* **10**: 2401-2410.
52. Sorensen, C. S., Syljuasen, R. G., Lukas, J., *et al.* (2004) ATR, Claspin and the Rad9-Rad1-Hus1- complex regulate Chk1 and Cdc25A in the absence of DNA damage. *Cell Cycle.* **3**: 941-945.
53. Cox, M. M., Goodman, M. F., Kreuzer, K. N., *et al.* (2000) The importance of repairing stalled replication forks. *Nature* **404**: 37-41.
54. Cox, M. M. (2002) The nonmutagenic repair of broken replication forks via recombination. *Mutation Research* **510**: 107-120.
55. Burtelow, M. A., Roos-Mattjus, P. M. K., Rauen, M., *et al.* (2001) Reconstitution and molecular analysis of the hRad9-hHus1-hRad1 (9-1-1) DNA damage responsive checkpoint complex. *The Journal of Biological Chemistry* **276**: 25903-25909.
56. Venclovas, C., and Thelen, M. P. (2000) Structure-based predictions of Rad1, Rad9, Hus1 and Rad17 participation in sliding clamp and clamp-loading complexes. *Nucleic Acids Research* **28**: 2481-2493.
57. Waga, S., and Stillman, B. (1998) The DNA replication fork in eukaryotic cells. *Annu. Rev. Biochem.* **67**: 721-751.
58. Mossi, R., and Hubscher, U. (1998) Clamping down on clamps and clamp loaders: The eukaryotic replication factor c. *Eur. J. Biochem.* **254**: 209-216.

59. Kelman, Z. (1997) PCNA: structure, functions and interactions. *Oncogene* **14**: 629-640.
60. Post, S. M., Tomlinson, A. E., and Lee, E. Y.-H. P. (2003) The human checkpoint Rad protein Rad17 is chromatin-associated throughout the cell cycle, localizes to DNA replication sites, and interacts with DNA polymerases. *Nucleic Acids Research* **31**: 5568-5575.
61. Roos-Mattjus, P., Vroman, B. T., Burtelow, M. A., *et al.* (2002) Genotoxin-induced Rad9-Hus1-Rad1 (9-1-1) chromatin association is an early checkpoint signaling event. *The Journal of Biological Chemistry* **277**: 43809-43812.
62. Furuya, K., Poitelea, M., Guo, L., *et al.* (2004) Chk1 activation requires Rad9 S/TQ-site phosphorylation to promote association with C-terminal BRCT domains of Rad4 TOPBP1. *Genes & Dev.* **18**: 1154-1164.
63. Guan, X., Madabushi, A., Chang, D. –Y., *et al.* (2007) The human checkpoint sensor Rad9-Rad1-Hus1 interacts with and stimulates DNA repair enzyme TDG glycosylase. *Nucleic Acids Research* **35**: 6207-6218.
64. Griffiths, D. J. F., Barbet, N. C., McCready, S., *et al.* (1995) Fission yeast rad17: a homologue of budding yeast RAD24 that shares regions of sequence similarity with DNA polymerase accessory proteins. *EMBO Journal* **14**: 5812-5823.
65. Rauen, M., Burtelow, M. A., Dufault, V. M., *et al.* (2000) The human checkpoint protein hRad17 interacts with the PCNA-like proteins hRad1, hHus1, and hRad9. *The Journal of Biological Chemistry* **275**: 29767-29771.
66. Caspari, T., Dahlen, M., Kanter-Smoler, G., *et al.* (2000) Characterization of *Schizosaccharomyces pombe* Hus1: a PCNA-related protein that associates with Rad1 and Rad9. *Molecular and Cellular Biology* **74**: 1254-1262.
67. Burtelow, M. A., Kaufmann, S. H., and Karnitz, L. M. (2000) Retention of the human Rad9 checkpoint complex in extraction-resistant nuclear complexes after DNA damage. *The Journal of Biological Chemistry* **275**: 26343-26348.
68. Bentley, N. J., Holtzman, D. A., Flaggs, G., *et al.* (1996) The *Schizosaccharomyces pombe rad3* checkpoint gene. *The EMBO Journal* **15**: 6641-6651.
69. Melo, J., and Toczyski, D. (2002) A unified view of the DNA-damage checkpoint. *Current Opinion in Cell Biology* **14**: 237-245.
70. Nyberg, K. A., Michelson, R. J., Putnam, C. W., *et al.* (2002) Toward maintaining the genome: DNA damage and replication checkpoints. *Annu Rev Genet* **36**: 617-656.
71. Edwards, R. J., Bentley, N. J., and Carr, A. M. (1999) A Rad3-Rad26 complex responds to DNA damage independently of other checkpoint proteins. *Nature Cell Biology* **1**: 393-398.
72. Wolkow, T. D., and Enoch, T. (2002) Fission yeast Rad26 is a regulatory subunit of the Rad3 checkpoint kinase. *Molecular Biology of the Cell* **13**: 480-492.
73. Harris, S., Kemplen, C., Caspari, T., *et al.* (2003) Delineating the position of *rad4*$^{+}$*/cut5*$^{+}$ within the DNA-structure checkpoint pathways in *Schizosaccharomyces pombe*. *Journal of Cell Science* **116**: 3519-3529.
74. Du, L.-L., Nakamura, T. M., Moser, B. A., *et al.* (2003) Retention but not recruitment of Crb2 at double-strand breaks requires Rad1 and Rad3 complexes. *Molecular and Cellular Biology* **23**: 6150-6158.

75. Narod, S. A., and Foulkes, W. D. (2004) *BRCA1* and *BRCA2*: 1994 and beyond. *Nature Reviews Cancer* **4**: 665-676.
76. Kai, M., and Wang, T. S.-F. (2003) Checkpoint responses to replication stalling: inducing tolerance and preventing mutagenesis. *Mutation Research* **532**: 59-73.
77. Lindsay, H. D., Griffiths, D. J. F., Edwards, R. J., *et al.* (1998) S-phase-specific activation of Cds1 kinase defines a subpathway of the checkpoint response in *Schizosaccharomyces pombe*. *Genes & Dev.* **12**: 382-395.
78. Zeng, Y., Forbes, K. C., Wu, Z., *et al.* (1998) Replication checkpoint requires phosphorylation of the phosphatase Cdc25 by Cds1 or Chk1. *Nature* **395**: 507-510.
79. Al-Khodairy, F., and Carr, A. M., (1992) DNA repair mutants defining G2 checkpoint pathways in *Schizosaccharomyces pombe*. *Embo J* **11**: 1343-1350.
80. Jimenez, G., Yucel, J., Rowley, R., *et al.* (1992) The *rad3*$^{+}$ gene of *Schizosaccharomyces pombe* is involved in multiple checkpoint functions and in DNA repair. *Proc. Natl. Acad. Sci. U.S.A.* **89**: 4952-4956.
81. Enoch, T., Carr, A. M., and Nurse, P. (1992) Fission yeast genes involved in coupling mitosis to completion of DNA replication. *Genes Dev.* **6**: 2035-2046.
82. Martinho, R. G., Lindsay, H. D., Flaggs, G., *et al.* (1998) Analysis of Rad3 and Chk1 protein kinases defines different checkpoint responses. *Embo J* **17**: 7239-7249.
83. Boddy, M. N., and Russell, P. (1999) DNA replication checkpoint control. *Frontiers of Bioscience* **4**: 841-848.
84. Stewart, E., Chapman, C. R., Al-Khodairy, F., *et al.* (1997) *rqh1*$^{+}$, a fission yeast gene related to the Bloom's and Werner's syndrome genes, is required for reversible S phase arrest. *Embo J* **16**: 2682-2692.
85. Liu, V. F., Bhaumik, D., and Wang, T. S. –F. (1999) Mutator phenotype induced by aberrant replication. *Mol Cell Biol* **19**: 1126-1135.
86. Osborn, A. J., Elledge, S. J., and Zou, L. (2002) Checking on the fork: the DNA-replication stress-response pathway. *TRENDS in Cell Biology* **12**: 509-516.
87. Paulsen, R. D., and Cimprich, K. A. (2007) The ATR pathway: fine-tuning the fork. *DNA Repair* **6**: 953-966.
88. Kai, M., Boddy, M. N., Russell, P., *et al.* (2005) Replication checkpoint kinase Cds1 regulates Mus81 to preserve genome integrity during replication stress. *Genes and Development* **19**: 919-932.
89. Lambert, S., Froget, B., and Carr, A. M. (2007) Arrested replication fork processing: interplay between checkpoints and recombination. *DNA Repair* **6**: 1042-1061.
90. Viguera, E., Hernandez, P., Krimer, D. B., *et al.* (2000) Visualisation of plasmid replication intermediates containing reversed forks. *Nucleic Acids Research* **28**: 498-503.
91. Postow, L., Ullsperger, C., Keller, R. W., *et al.* (2001) Positive torsional strain causes the formation of a four-way junction at replication forks. *J Biol Chem* **276**: 2790-2796.
92. Carr, A. M. (1997) Control of the cell cycle arrest by the Mec1^{sc}/Rad3^{sp} DNA structure checkpoint pathway. *Curr Opin Genet Dev* **7**: 93-98.
93. Carr, A. M. (2002) DNA structure dependent checkpoints as regulators of DNA repair. *DNA Repair* **1**: 983-994.

94. Khakhar, R. R., Cobb, J. A., Bjergbaek, L., *et al.* (2003) RecQ helicases: multiple roles in genome maintenance. *TRENDS in Cell Biology* **13**: 493-501.
95. Doe, C. L., Ahn, J. S., Dixon, J., *et al.* (2002) Mus81-Eme1 and Rqh1 involvement in processing stalled and collapsed replication forks. *J Biol Chem* **277**: 32753-32759.
96. Boddy, M. N., Shanahan, P., McDonald, W. H., *et al.* (2003) Replication checkpoint kinase Cds1 regulates recombinational repair protein Rad60. *Mol Cell Biol* **23**: 5939-5946.
97. Morishita, T., Tsutsui, Y., Iwasaki, H., et al. (2002) The Schizosaccharomyces pombe rad60 gene is essential for repairing double-strand DNA breaks spontaneously occurring during replication and induced by DNA-damaging agents. *Mol Cell Biol* **22**: 3537-3548.
98. Murray, J. H., Lindsay, H. D., Munday, C. A., *et al.* (1997) Role of *Schizosaccharomyces pombe* RecQ homolog, recombination, and checkpoint genes in UV damage tolerance. *Mol Cell Biol* **17**: 6868-6875.
99. Kai, M., and Wang, T. S. –F. (2003) Checkpoint activation regulates mutagenic translesion synthesis. *Genes Dev.* **1**: 64-76.
100. Win, T. Z., Mankouri, H.W., Hickson, I. D., *et al.* (2005) A role for the fission yeast Rqh1 helicase in chromosome segregation. *J Cell Sci* **118**: 5777-5784.
101. Doe, C. L., Dixon, J., Osman, F., *et al.* (2000) Partial suppression of the fission yeast *rqh1*$^-$ phenotype by expression of a bacterial Holliday junction resolvase. *EMBO J* **19**: 2751-2762.
102. Boddy, M. N., Lopez-Girona, A., Shanahan, P., *et al.* (2000) Damage tolerance protein Mus81 associates with the FHA1 domain of checkpoint kinase Cds1. *Mol Cell Biol* **20**: 8758-8766.
103. Kalirman, V., Mullen, J. R., Fricke, W. M., *et al.* (2001) Functional overlap between Sgs1-Top3 and the Mms4-Mus81 endonuclease. *Genes Dev* **15**: 2730-2740.
104. Boddy, M. N., Gaillard, P. –H. L., McDonald, W. H., *et al.* (2001) Mus81-Eme1 are essential components of a holliday junction resolvase. *Cell* **107**: 537-548.
105. Bastin-Shanower, S. A., Fricke, W. M., Mullen, J. R., *et al.* (2003) The mechanism of Mus81-Mms4 cleavage site selection distinguishes it from the homologous endonuclease Rad1-Rad10. *Molecular and Cellular Biology* **23**: 3487-3496.
106. Chakraverty, R. K., and Hickson, I. D. (1999) Defending genome integrity during DNA replication: a proposed role for RecQ family helicases. *BioEssays* **21**: 286-294.
107. Davey, S., Han, C. S., Ramer, S. A., *et al.* (1998) Fission yeast *rad12*$^+$ regulates cell cycle checkpoint control and is homologous to the Bloom's syndrome disease gene. *Mol Cell Biol* **18**: 2721-2728.
108. Karow, J. K., Constantinou, A., Li, J. –L., *et al.* (2000) The Bloom's syndrome gene product promotes branch migration of Holliday junctions. *PNAS* **97**: 6504-6508.
109. Hickson, I. D., Davies, S. L., Li, J. L., *et al.* (2001) Role of the Bloom's syndrome helicase in maintenance of genome stability. *Biochem Soc Trans* **29**: 201-204.

110. Laursen, L. V., Ampatzidou, E., Andersen, A. H., *et al.* (2003) Role for the fission yeast RecQ helicase in DNA repair in G(2). *Mol Cell Biol* **23**: 3692-3705,
111. Wu, L., and Hickson, I. D. (2002) RecQ helicases and cellular responses to DNA damage. *Mutat Res* **509**: 35-47.
112. Frei, C., and Gasser, S. M. (2000) RecQ-like helicases: the DNA replication checkpoint connection. *J Cell Sci* **113**: 2641-2646.
113. Constantinou, A., Tarsounas, M., Karow, J. K., *et al.* (2000) Werner's syndrome protein (WRN) migrates Holliday junctions and co-localizes with RPA upon replication arrest. *EMBO Reports* **1**: 80-84.
114. Fabre, F., Chan, A., Heyer, W. D., *et al.* (2002) Alternate pathways involving Sgs1/Top3, Mus81/Mms4, and Srs2 prevent formation of toxic recombination intermediates from single-stranded gaps created by DNA replication. *PNAS* **99**: 16887-16892.
115. Chua, G., Taricani, L., Stangle, W., *et al.* (2000) Insertional mutagenesis based on illegitimate recombination in *Schizosaccharomyces pombe*. *Nucleic Acids Research* **28**: e53 i-vi.
116. Hoffman, C. S., and Welton, R. (2000) Mutagenesis and gene cloning in *Schizosaccharomyces pombe* using nonhomologous plasmid integration and rescue. *Biotechniques* **28**: 532-536, 538, 540.
117. Sambrook, J., Fritsch, E. F., and Maniatis, T. (1989) *Molecular Cloning: A Laboratory Manual 2nd Ed.,* Cold Spring Harbor Laboratory Press, Cold Spring Harbor.
118. Okazaki, K., Okazaki, N., Kume, K., *et al.* (1990) High-frequency transformation method and library transducing vectors for cloning mammalian cDNAs by trans-complementation of *Schizosaccharomyces pombe. Nucleic Acids Research* **18**: 6485-6489.
119. Moreno, S., Klar, A., and Nurse, P. (1991) Molecular genetic analysis of fission yeast *Schizosaccharomyces pombe*. *Methods Enzymol* **194**: 795-823.
120. Grimm, C., Kohli, J., Murray, J., *et al.* (1988) Genetic engineering of *Schizosaccharomyces pombe*: A system for gene disruption and replacement using the *ura4* gene as a selectable marker. *Mol Gen Genet* **215**: 81-86.
121. Davidson, M. K., Young, N. P., Glick, G. G., *et al.* (2004) Meiotic chromosome segregation mutants identified by insertional mutagenesis of fission yeast *Schizosaccharomyces pombe*; tandem-repeat, single-site integrations. *Nucleic Acids Research* **32**: 4400-4410.
122. Rodriguez-Gabriel, M. A., Burns, G., McDonald, W. H., *et al.* (2003) RNA-binding protein Csx1 mediates global control of gene expression in response to oxidative stress. *EMBO Journal* **22**: 6256-6266.
123. Ahmad, M., and Bussey, H. (1986) Yeast arginine permease: nucleotide sequence of the CAN1 gene. *Curr Genet* **10**: 587-592.
124. Rosenthal, G. A. (1977) The biological effects and mode of action of L-canavanine, a structural analogue of L-arginine. *Q Rev Biol* **52**: 155-178.
125. Ayoub, N., Noma, K., Isaac, S., *et al.* (2003) A novel jmjC domain protein modulates heterochromatization in fission yeast. *Molecular and Cellular Biology* **23**: 4356-4370.

126. Dai, Z. –M., Zhu, X. –J. Chen, Q., *et al.* (2007) PCR-suppression effect: kinetic analysis and application to representative or long-molecule biased PCR-based amplification of complex samples. *Journal of Biotechnology* **128**: 435-443.
127. Collins, F. S., and Weissman, S. M. (1984) Directional cloning of DNA fragments at a large distance from an initial probe: a circularization method. *PNAS* **81**: 6812-6816.
128. Shagin, D. A., Lukyanov, K. A., Vagner, L. L., *et al.* (1999) Regulation of average length of complex PCR product. *Nucleic Acids Research* **27**: e23i-iii.